

An Attempt to Formulate Non-Carbonate Electrolytes for Sodium-Ion Batteries

Ronnie Mogensen,^[a] Simon Colbin,^[a] and Reza Younesi^{*[a]}

Non-aqueous carbonate solvents have been the main choice for the development of lithium-ion batteries, and similarly most research on sodium-ion batteries have been performed using carbonate-based solvents. However, the differences between sodium and lithium batteries – in term chemistry/electrochemistry properties as well as electrode materials used – open up opportunities to have a new look at solvents that have attracted little attention as electrolyte solvent. This work investigates properties of a wide range of different solvent classes in the context of sodium-ion battery electrolytes and compares them to the performance of propylene carbonate. The thirteen solvents studied here include one or several members of glymes, carbonates, lactones, esters, pyrrolidones, sulfones, and alkyl phosphates. Out of those, five outperforming solvents of γ -butyrolactone (GBL), γ -valerolactone (GVL), *N*-methyl-2-pyrrolidone (NMP), propylene carbonate (PC), and

trimethyl phosphate (TMP) were further investigated using additives of ethylene sulfite (ES), vinylene carbonate (VC), fluoroethylene carbonate (FEC), prop-1-ene-1,3-sultone (PES), sulfolane (TMS), tris(trimethylsilyl) phosphite (TTSPi), and sodium bis(oxalato)borate (NaBOB). The solvents TMS and tetraethylene glycol dimethyl ether (TEGDME) were tested in 1:1 mixtures by volume with the co-solvents; NMP, dimethoxyethane (DME), and TMP. All electrolytes used NaPF₆ as the salt. Primary evaluation relied on electrochemical cycling of full-cell sodium-ion batteries consisting of Prussian white cathodes and hard-carbon anodes. Galvanostatic cycling was performed using both two- and three-electrode cells, in addition, cyclic and linear sweep voltammetry was used to further evaluate the electrolyte formulations. Moreover, the resistance was measured on the anode and cathode, using Intermittent current interruption (ICI) technique.

1. Introduction

Sodium-ion batteries (SIBs) have become an established technology in the battery research field following a decade of intensive research efforts. As a result, there are now several interesting anode and cathode materials that are viable and realistic candidates for commercialization.^[1–3] The majority of the research in SIBs have used analogues of the carbonate electrolytes currently used in lithium-ion batteries (LIBs). Therefore, it remains an open question if the decades of trial and error in developing these electrolytes for LIBs^[4,5] will provide the best results for SIBs. Today, it is apparent that the electrolyte is one of the main obstacles to commercialization of SIBs.^[6–9] This statement does not only refer to performance in the batteries themselves, but also to the cost, safety and environmental-sustainability of the materials used in the electrolytes.^[10,11] Despite the ever increasing amount of work on SIB electrolytes, many solvents are not well explored, since most work has been focused on ethers and carbonates. A cohesive and comprehensive picture of the options is needed.

We should beware of only selecting candidates based on what LIBs uses and instead take a fresh and unbiased look at all the alternatives.

Many solvents have been disqualified in early SIB research due to their incompatibility with sodium-metal. Similarly, many promising solvent candidates for LIBs were considered unpractical due to their incompatibility with graphite and then virtually forgotten. Graphite is not the premier anode material in SIBs, and sodium-metal is ideally not present in rocking-chair-type batteries, thus making the traditional criteria for conventional formulations less relevant. To develop new electrolytes for SIBs, we revisit the solvent-list of LIB history, and reexamine the performance of old and new candidates combined with the NaPF₆ salt. Unsurprisingly, this work has intentionally avoided the use of sodium metal in all cells, except for the cyclic voltammetry tests. This means that more solvents could be included and issues related to side products formed by sodium metal can be avoided.

All the electrolytes in this work were subjected to testing in a well-defined and standardized manner, using two- and three-electrode full-cells; replicate cells were used to improve the reliability of the results. The full-cells were comprised of Prussian white cathodes and hard-carbon anodes due to their performance and good stability. We also combined a selection of the tested solvents with some of the most commonly used additives to leverage the progress made in electrolytes in the recent years. Our work aims to provide a comparative data set, including a wide range of solvents and additives tested under identical conditions.

[a] Dr. R. Mogensen, S. Colbin, Assoc. Prof. R. Younesi
Department of Chemistry – Ångström Laboratory
Uppsala University
Box 538, 75121 Uppsala, Sweden
E-mail: reza.younesi@kemi.uu.se

 Supporting information for this article is available on the WWW under
<https://doi.org/10.1002/batt.202000252>

 © 2020 The Authors. *Batteries & Supercaps* published by Wiley-VCH GmbH.
This is an open access article under the terms of the Creative Commons Attribution License, which permits use, distribution and reproduction in any medium, provided the original work is properly cited.

We first establish a baseline for a large amount of solvents without additives. Some of the solvent candidates were then chosen for further exploration with additives and co-solvents. The baseline characterization included conductivity measurements of all additive-free electrolytes for concentrations close to 0.5, 1, and 1.5 M NaPF₆. The electrolytes with salt concentrations corresponding to the highest conductivity were tested by cyclic and linear sweep voltammetry to elucidate the electrochemical stability. Following this, all the electrolytes were evaluated by galvanostatic cycling in full-cells. After the initial tests, more in-depth testing was performed for selected solvents. This selection process is schematically described in Figure 1.

The solvents chosen for use with additives were selected due to their good physical properties such as a wide liquid temperature window and high ionic conductivity, while less emphasis was put on their cycling performance. The rationale is that additives might improve the cycling performance, but they will not significantly change the physical properties of the solvent. The solvents were combined into binary mixtures when cycling performance was promising, despite poor physical properties. Solvents with high viscosity and high

boiling point were here combined with solvents of low viscosity and low boiling point.

The article contains the most important and revealing results. However, a large part is moved to the Supporting Information since the amount of collected data is rather large. We therefore strongly encourage the reader to look at the Supporting Information to get the full results and detailed information of each sample.

2. Results and Discussion

Characterization of the electrolytes started with ionic conductivity measurements of each solvent. Measurements were performed at room temperature on electrolytes close to 0.5, 1, and 1.5 M NaPF₆ (Tables S1 and S2). Several solvents did not reach their maximum ionic conductivity within the concentration span. Still, increasing the concentration further would bring the work into the field of highly concentrated electrolytes which is beyond the scope of this study.

The maximum ionic conductivity achieved for each solvent is presented in Figure 2a together with the viscosity and dielectric constant for the salt-free solvents,^[12–21] while the

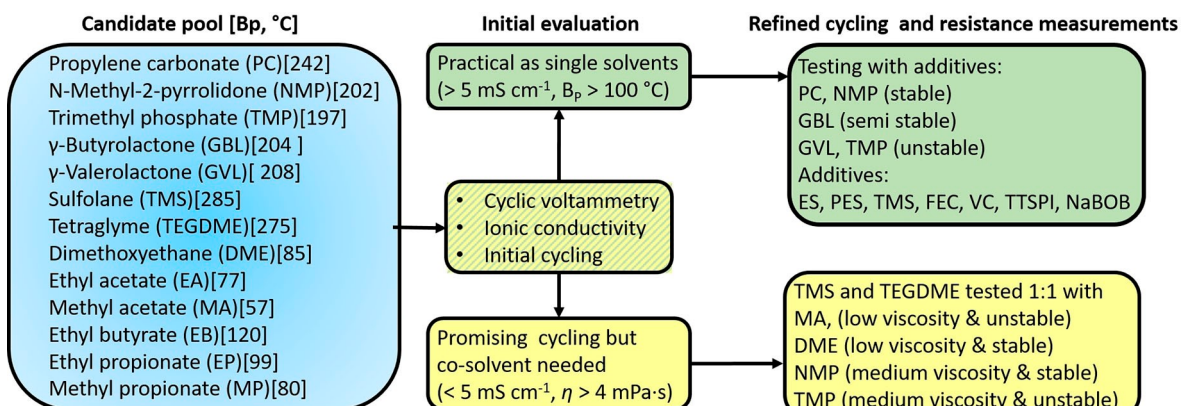


Figure 1. A flowchart describing the solvent selection process for performance and resistance tests with additives and co-solvents.

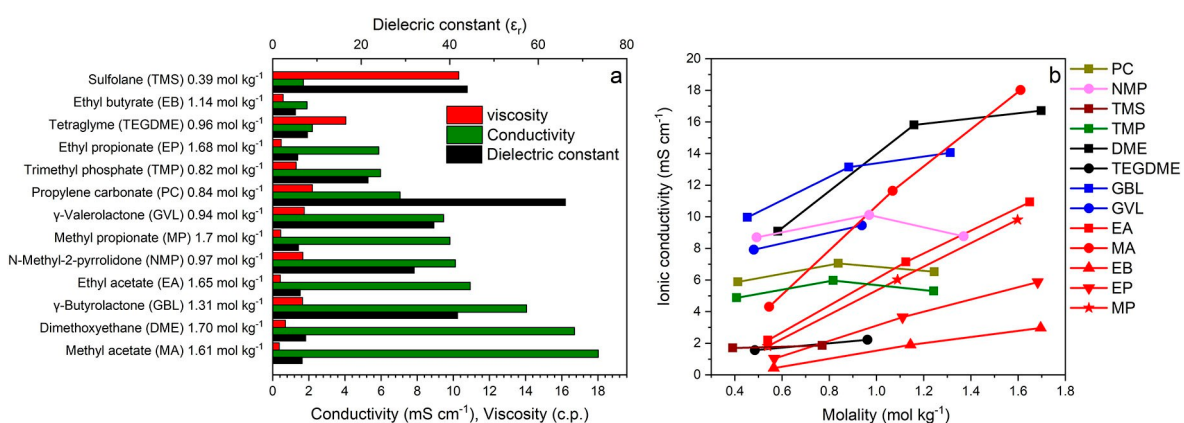


Figure 2. Dielectric constant and viscosity for salt-free solvents,^[12–21] compared with the maximum achieved ionic conductivity at room temperature for all the tested solvents (a). The ionic conductivity as a function of the NaPF₆ concentration in molal for all the tested solvents (b).

conductivity as a function of concentration is displayed in Figure 2b.

Both methyl acetate (MA) with 1.61 molal NaPF_6 and dimethoxyethane (DME) with 1.70 molal NaPF_6 surpass ionic conductivities of 16 mScm^{-1} , while ethyl butyrate (EB), tetra-ethylene glycol dimethyl ether (TEGDME) and sulfolane (TMS) stand out as the solvents with the lowest conductivities. As evidenced in Figure 2, neither viscosity, the class of solvent, nor the dielectric constant seem to be a very useful predictors of ionic conductivity when using a weakly associating anion such as PF_6^- ; from the presented data the only conclusion can be that predicting ionic conductivity from viscosity and dielectric constant alone is rather difficult. It is worth noting the capability of esters to dissolve large amounts of NaPF_6 without lowered conductivity (Figure 2b) since this could make them prime candidates for high-concentration electrolyte studies.

A simple submersion test of metallic sodium in each electrolyte was conducted using a freshly cleaned sodium piece in a glovebox. In this test, the glymes (DME, TEGDME) together with trimethyl phosphate (TMP) and γ -butyrolactone (GBL) showed no visible reaction. Ethyl propionate (EP) and EB, together with *N*-methyl-2-pyrrolidone (NMP) showed severe reactions with metallic sodium, whereas the remaining solvents displayed moderate reactivity (Table S3).

The electrochemical stability window was determined for electrolytes, using concentrations corresponding to their max-

imum ionic conductivity (see Figure 3). Cyclic and linear sweep voltammetry was performed using discs of carbon-coated aluminum as working electrodes. Note that metallic sodium was used as a counter electrode and reaction products from the counter electrode could thus have influenced the results. The full results of the cyclic and linear sweep voltammetry are available in the supplemental information (Supporting Information, see Part 4).

A relatively high oxidation stability (up to 4 volts vs. Na^+/Na) was shown for electrolytes based on propylene carbonate (PC), TEGDME, DME, and TMP (Figure 3a); whereas GBL and γ -valerolactone (GVL) suffer from severe oxidation at potentials above 3 V (Figure 3c). TMS and NMP both show lacking oxidation stability above 2 volts, however, for TMS the oxidation current is less substantial (Figure 3b,c). The esters are unstable to varying degrees in regards to oxidation, but all display significant currents well below 4 V (Figure 3d). Based on the cyclic voltammetry, many electrolytes seemed unlikely to survive cycling up to 4 V in full-cells. Nevertheless, most electrolytes presented in Figure 3 delivered more than 60 mAhg^{-1} in full-cells using hard-carbon anodes and Prussian white cathodes. The results from representative cells are presented in Figure 4; all replicate cells details are available in the Supporting Information, Tables S4, S5, and S6.

As expected, the commonly used solvents PC, DME, and TEGDME performed well, with 76%, 80%, and 72% initial

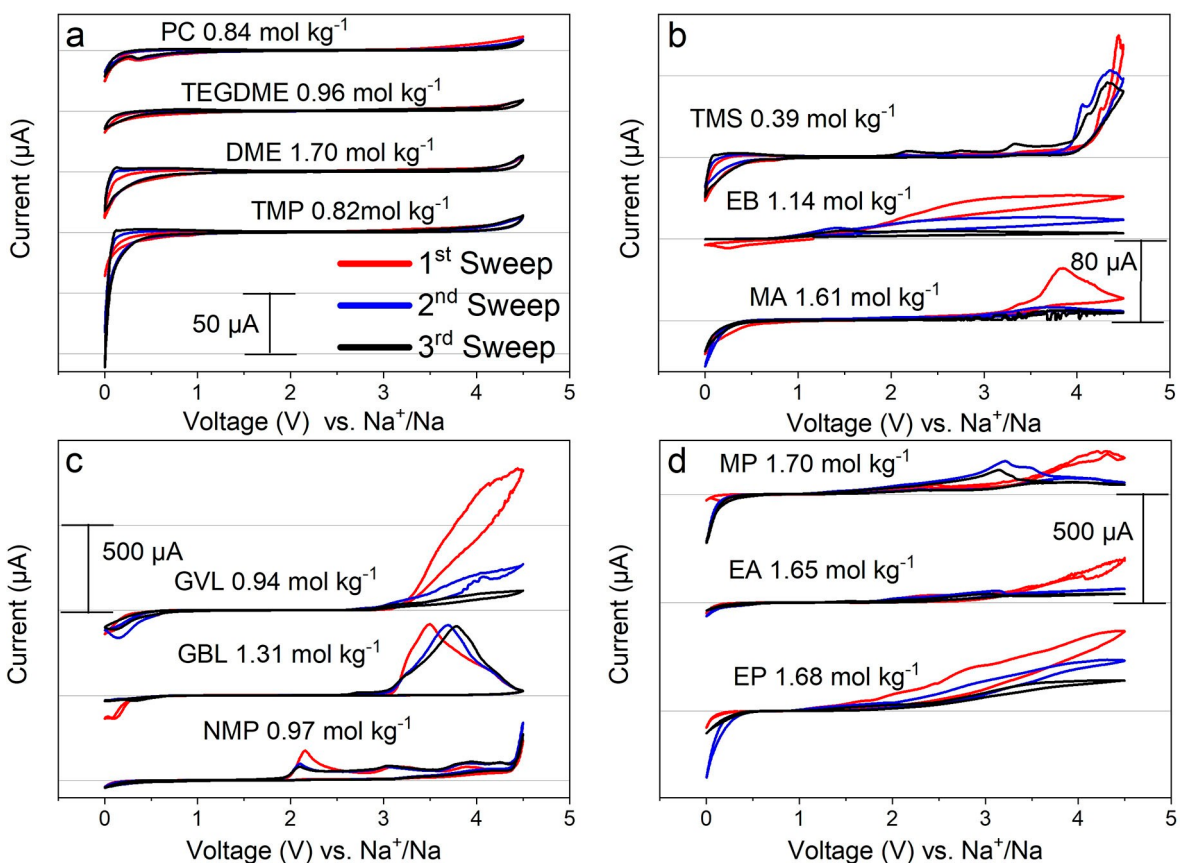


Figure 3. Cyclic voltammetry of different solvent using the NaPF_6 salt. The concentrations correspond to the respective maximum ionic conductivity. Voltage limits were set to 0.001 and 4.5 V vs. Na^+/Na , and scan speed was set to 1 mVs^{-1} .

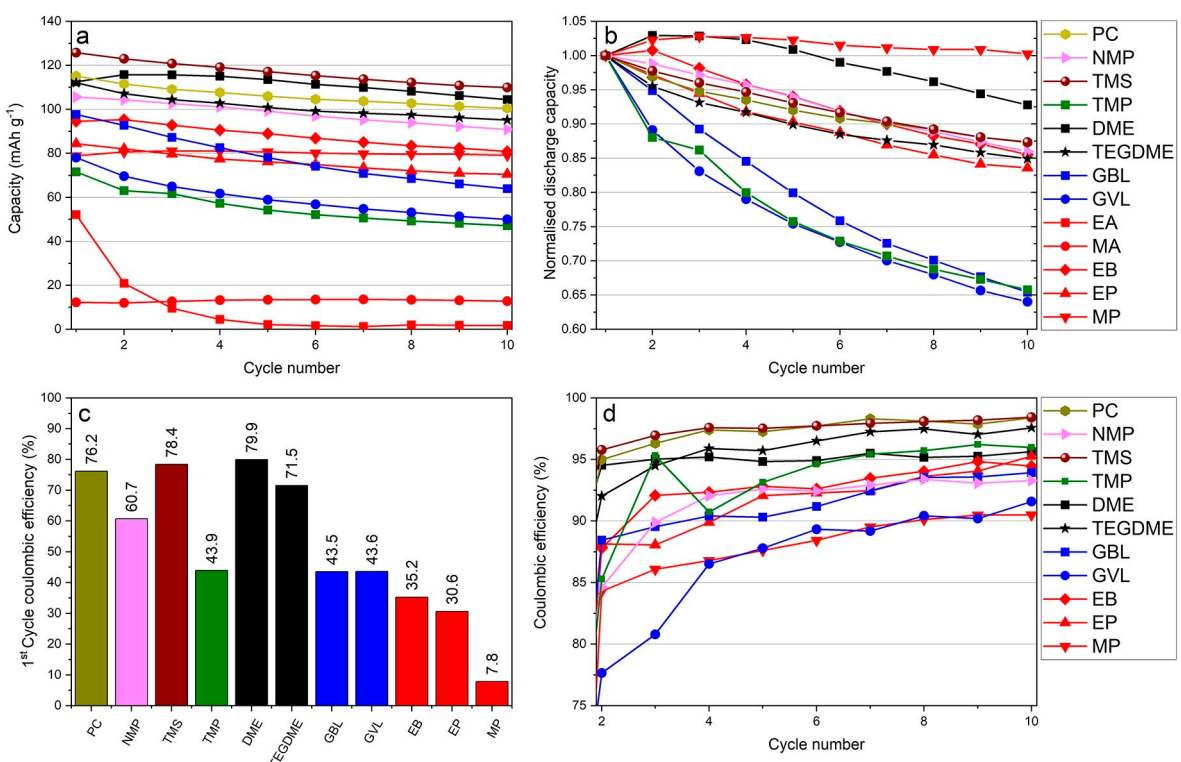


Figure 4. Galvanostatic cycling of two-electrode sodium-ion full-cells using Prussian white (PW) cathodes and hard carbon (HC) anodes; showing the discharge capacity in mAh g^{-1} (cathode) (a) and normalized vs. the first discharge (b), with the initial Coulombic efficiency (ICE) (c) and Coulombic efficiency (CE) for the remaining 9 cycles (d). Cycling was performed at 30 mA g^{-1} between 2 V and 4 V.

Coulombic efficiency (ICE), respectively (see Figure 4c). TMS achieved 78% ICE and retained 110 mAh g^{-1} capacity after the 10th cycle, whereas the corresponding numbers for NMP were 61% ICE and 91 mAh g^{-1} retention. EB displayed severe side reactions during charge that resulted in a low ICE, 35%. Interestingly, EB still displayed similar capacity fading as the previously mentioned electrolytes. Methyl propionate (MP) stands out with extremely good capacity retention, although the horrible ICE (7.82%) means that there must be severe side reactions occurring in the cell; it is thus not a viable electrolyte without additives.

The remaining solvents include both some of the best and worst performers from cyclic voltammetry. EP had a low ICE, but exhibited better capacity retention than GBL, GVL, and TMP, while MA and ethyl acetate (EA) showed poor cycling performance. The initial results indicate that carbonates, sulfones and ethers represented by PC, TMS, DME, and TEGDME were compatible with hard-carbon since they all achieved ICE values above 70%. Electrolytes using the solvents NMP, GVL, GBL, and TMP showed intermediate performance and were plagued by side reactions which indicates that the solid-electrolyte interface (SEI) was not well formed. The acetate esters showed little promise as single solvents, whereas the butyrate and propionate esters: EB, EP, and MP, cycled better than GVL, GBL, and TMP despite low ICE values in the range of 8–35%.

2.1. Additives and Co-Solvents

A selection of five solvents were chosen for optimization with additives (see Figure 5). The solvents: PC, NMP, TMP, GBL, and GVL, were individually combined with six different additives in the following concentrations: PES 2 wt% (PES: prop-1-ene-1,3-sultone), TTSPI 2 vol% (TTSPI: tris(trimethylsilyl) phosphite), ES 5 vol% (ES: ethylene sulfite), TMS 5 vol%, FEC 2 vol% (FEC: fluoroethylene carbonate), VC 2 vol% (VC: vinylene carbonate), NaBOB 2 wt% (NaBOB: sodium bis(oxalato)borate) or less depending on solubility (see Table S7). In addition, binary mixtures using 1:1 ratio with either TEGDME or TMS as one component in combination with TMP, NMP, DME, and MA, were investigated (see Figure 6). 1 M NaPF_6 was used in all the electrolytes.

The testing consisted of at least two replicates of two-electrode full-cells (Prussian white-hard carbons) per electrolyte, and one three-electrode cell. The three-electrode cells also used intermittent current interruption (ICI) measurements, where the reference was a Prussian white electrode desodiated to 3.3 V vs. $\text{Na}^+/\text{Na}^{[22]}$. The ICI technique used a galvanostatic cycling program with short-duration (1 second) intermittent current interruptions that is used to measure internal resistance of the electrodes during cycling at five-minute intervals. A full explanation of the technique and examples of its implementation can be found in the works by Lacey et al.^[23,24]

The results presented below is collected from representative cells between cycles 1–10 at the current density of

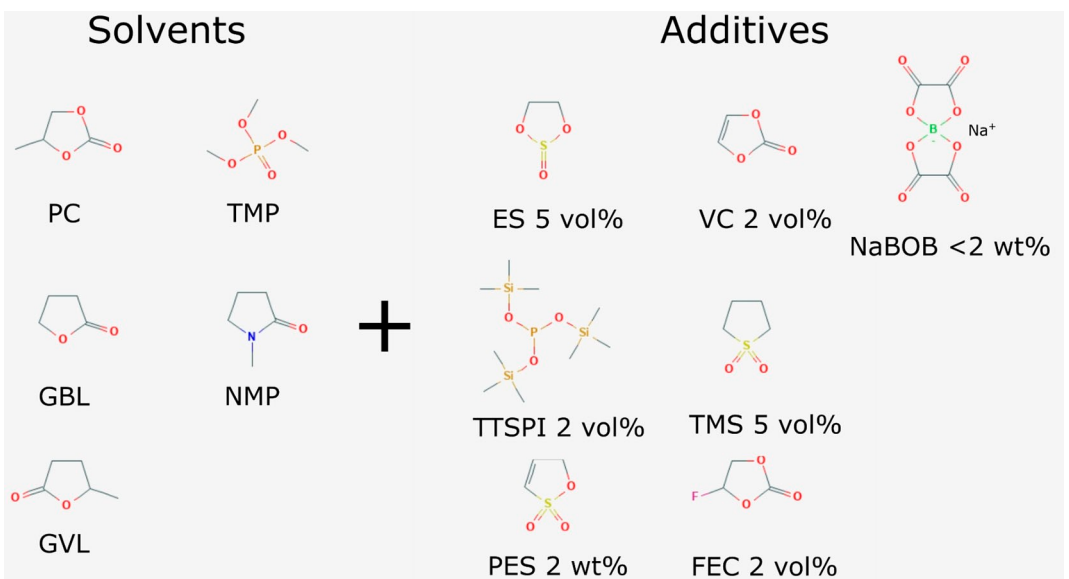


Figure 5. Overview of the test matrix, where each solvent was combined with each additive in a setup combining one single solvent and one single additive with 1 M NaPF_6 . Galvanostatic cycling in two- and three-electrode cells using PW cathodes and hard carbon anodes were applied to evaluate the electrolytes.

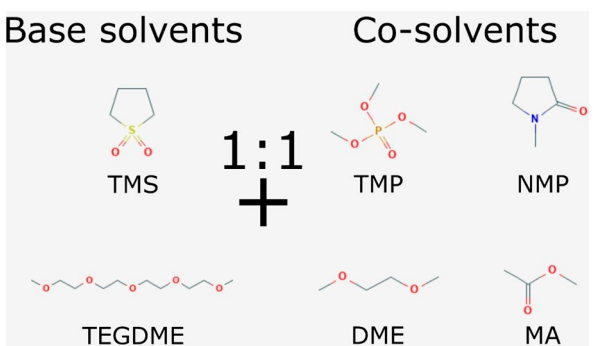


Figure 6. Overview for the tests of binary electrolytes. TMS was tested in mixtures corresponding to 1:1 by volume with TMP, NMP, DME, and MA, while TEGDME was combined with TMP, NMP, and DME. All the binary electrolytes used 1 M NaPF_6 and was tested by galvanostatic cycling in two and three-electrode cells using Prussian white cathodes and hard carbon anodes.

30 mA g^{-1} for both two- and three-electrode cells. The two-electrode cells were cycled for an additional 10 cycles at a current density of 150 mA g^{-1} . When the average is stated, it is collected from the combined cell-data from all the replicates. It should be noted that for practical reasons two-electrode cells were cycled with only vacuum providing the stack pressure, while three-electrode cells were cycled with clamps and plates that provided additional stack pressure. All the individual cell data is available in the Supporting Information.

2.1.1. Solvents

2.1.1.1. Propylene Carbonate (PC)

PC is one of the most common solvents in SIB research. It has many attractive properties, such as low toxicity, good electrochemical stability, and wide temperature limits.^[25] One significant downside of PC is its relatively high viscosity compared to the EC:DEC mixtures that are commonly used in LIB research.^[14] PC, although far from perfect, provides a baseline for the testing system and the additives used. The abundance of literature available on PC electrolyte mixtures can reveal any issues that relates to other components in the test system.^[14,25–29,30]

PC showed good stability in both cyclic and linear sweep voltammetry even when sodium metal was present in the cell. This is in contrast to the observation that PC is not particularly effective in stripping and plating of sodium.^[31] Regardless, additive-free PC achieved a satisfactory average ICE of 80.3%, but the cells showed rapid capacity fading (see Figure 7). The average discharge capacity starts at 126 mAh g^{-1} and drops to 104 mAh g^{-1} by the 10th cycle, and after ten additional cycles at 150 mA g^{-1} , only 78 mAh g^{-1} average discharge capacity remains for the two best cells. The energy efficiency for additive-free PC was consistently above 90%. It is thus in the range of acceptable levels for energy storage devices. It is, however, known that pure PC- NaPF_6 is far from a stable system. Our results confirm that the capacity fading was severe and the reference potentials shifted due to spontaneous sodiation of the Prussian white reference electrode. Furthermore, additive-free PC showed larger variations between cells compared to most other systems despite the promising ICE.

The cycling stability of PC is significantly improved when using additives (Figure 7). Yet, the ICE was only improved by a

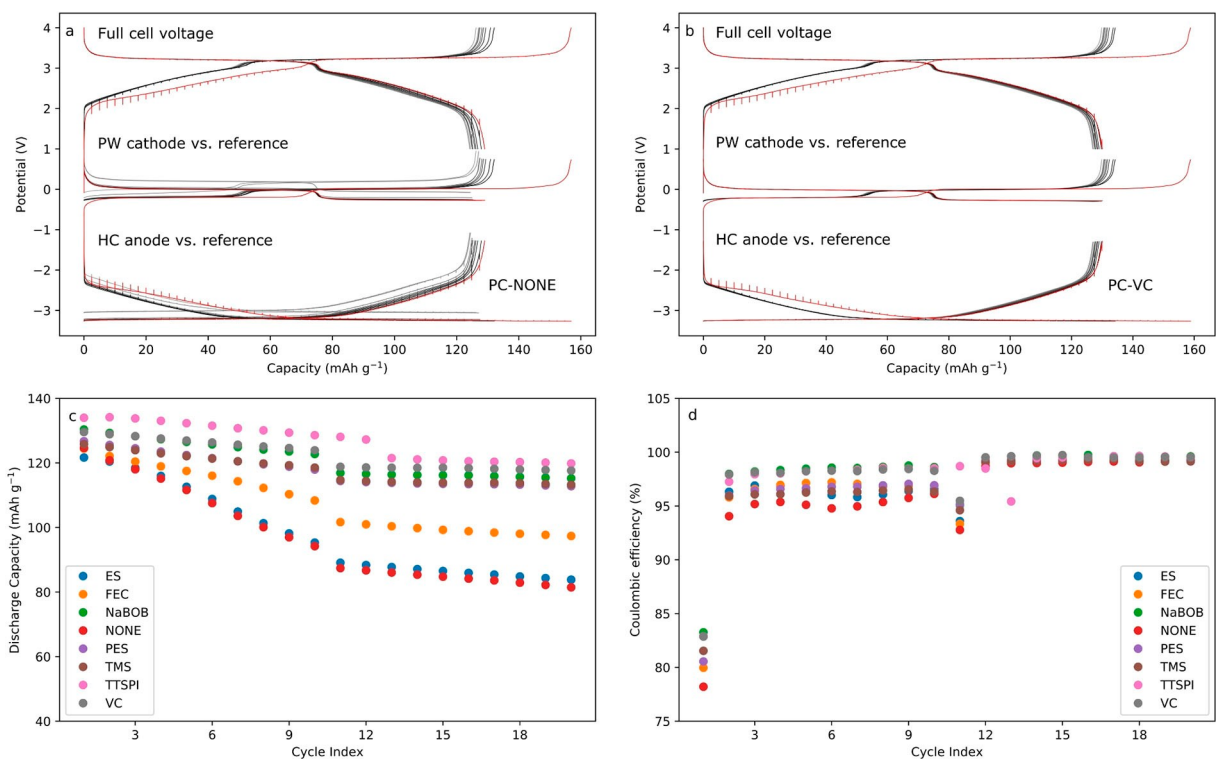


Figure 7. Galvanostatic cycling for ten cycles of three-electrode cells using 1 M NaPF₆ in PC without additive (a) and with 2 vol % VC (b). Three electrode cells used a PW reference electrode at 3.3 V vs. Na⁺/Na. Discharge capacities (c) and Coulombic efficiencies (d) of 1 M NaPF₆ in PC electrolytes with different additives cycled in two-electrode full-cells at the current density of 30 mA g⁻¹ for the first ten cycles and 150 mA g⁻¹ for the subsequent ten cycles.

few percent even by the best performing additives. The obtained average values ICE-values were: 81.2% (FEC), 81.2% (VC), 82.8% (NaBOB), 80.2% (PES), and 82.9% (TMS). The CE for additive free PC electrolyte stabilizes at around 95% at a low current density (30 mA g⁻¹), it is significantly higher at 150 mA g⁻¹ indicating that time-dependent parasitic reactions are occurring. This was also the case for most additives. Still, a significantly higher CE was observed at slow rates when using NaBOB and VC, indicating a reduced rate dependence. Furthermore, all additives significantly reduced the reference electrode drift in the three-electrode cells. In addition, VC, TTSPi, TMS, PES, and NaBOB significantly improved the capacity retention, and raised the energy efficiency to approximately 95%. Overall, every additive provided a capacity retention increase. The best performing additive for PC was VC. That is, VC had by a small margin the most positive effect on ICE, average CE, capacity retention, and energy efficiency.

We obtained indirect information regarding the SEI formation by tracking the resistance evolution during the first charge (Figure 8). ICL measures the electrode resistance; the deposition of an SEI affects this resistance. However, a rather large background was present. This was due to the bulk resistance of the electrode, which changes with state-of-charge. Regardless, additive-free PC displayed a double peak in resistance measurement during the initial SEI formation. This was also present when using NaBOB and TMS additives. ES, FEC, PES, and VC all increased the initial resistance and interfered with the decomposition of PC, which in turn

obscured the characteristic double resistance peak displayed by additive-free PC. By the end of the charge, most of the additives stabilized at roughly the same resistance. Yet there were two notable exceptions: 1) ES initially showed a higher resistance on the anode during the first charge, with reduced resistance as cycling progresses (Figure 8b). 2) TTSPi exhibited the lowest resistance of all PC formulations by the end of the first charge, but displayed increasing resistance as cycling progressed (Figure 8d). The fact that all additives somewhat improve the cycling performance of PC is likely due to selection bias of the additives since many additives are specifically developed for carbonate solvents.

2.1.1.2. γ -Butyrolactone (GBL)

GBL is interesting for electrolytes due to its stellar physical properties and high ionic conductivity. It has been investigated in the early days of LIB research and is still a hot subject for research as an electrolyte.^[32-37] GBL has a superb liquid temperature range (-44 °C to 204 °C)^[33] and an ionic conductivity of 14.05 mS cm⁻¹ at 1.31 molal NaPF₆. This is almost twice of ionic conductivity of 0.84 molal NaPF₆ in PC which is equal to 7.05 mS cm⁻¹. Despite the good properties of GBL, only one recent work was found in literature regarding sodium-ion batteries; in this work the GBL-based electrolyte was shown to suffer from severe degradation when cycled above 3.9 V vs. Na⁺/Na, when using the novel salt sodium bis(salicylato)

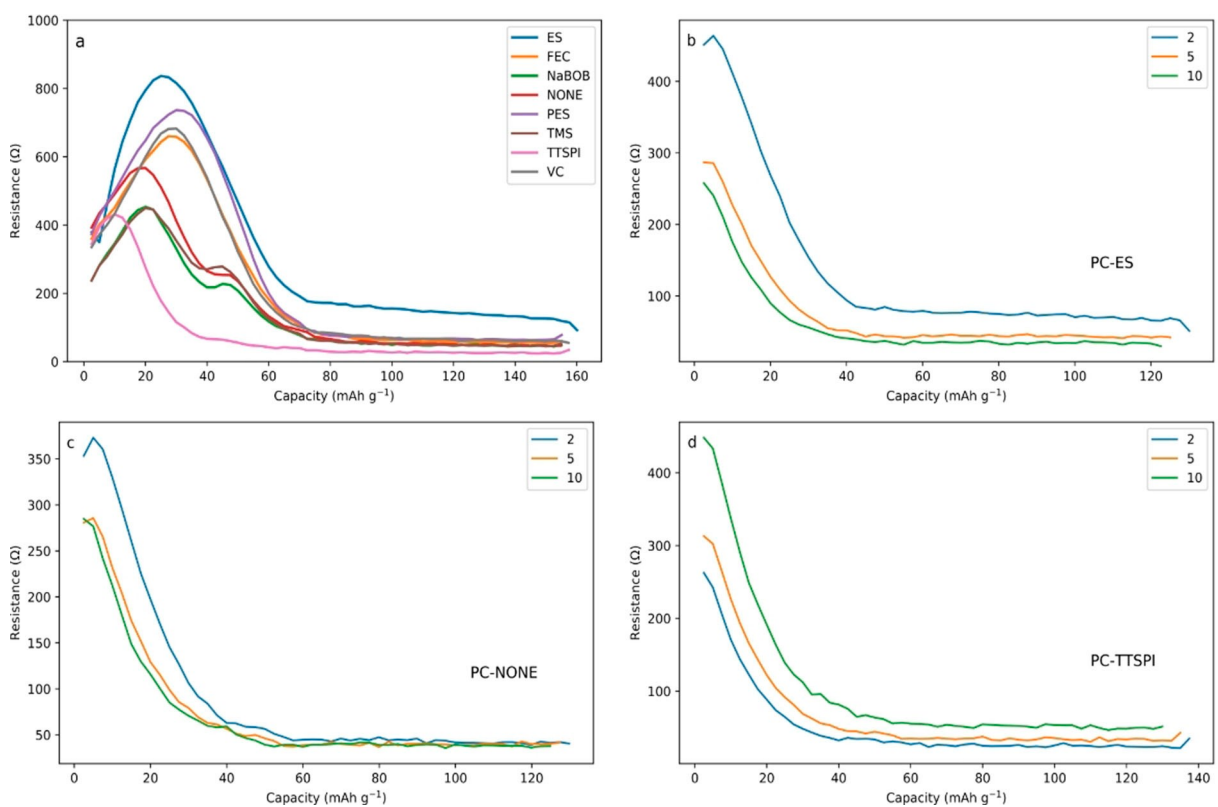


Figure 8. Resistance of the hard-carbon electrode during the 1st charge for all PC electrolyte formulations (a), with the resistance during the 2nd, 5th, and 10th cycle charge for PC-ES (b), Additive-free PC(c), and PC-TTSPI formulations (d).

borate.^[38] The cyclic voltammetry of GBL in this work similarly indicated lacking oxidative stability, where an oxidation occurred at 3 V vs. Na⁺/Na with no signs of passivation. Yet this was not fully reflected in our cell cycling results (see Figure 9). The average ICE from three additive-free GBL was 73.6 %. This is significantly lower than what was obtained for additive-free PC electrolyte. However, the additive-free GBL showed promising cycling with an average 20th cycle retention of 99.5 mAh g⁻¹, and thus outperformed additive-free PC by approximately 20%.

GBL was moderately affected by additives in terms of capacity retention. However, the cycling revealed that several additives did increase the energy efficiency. NaBOB, PES, and VC all improved the ICE of GBL while the other additives had a detrimental impact. The best improvement was obtained using PES. Here an ICE of 80.2 % was achieved and thus raised the ICE by 6.6 %. In addition, the average discharge capacity of the 20th cycle was increased from 99 mAh g⁻¹ to 106 mAh g⁻¹ in the cell with PES compared to the additive-free cell.

Additive-free GBL and additive-free PC behaved similarly. The CE was strongly rate dependent, ca. 95 % CE at 30 mA g⁻¹ and ca. 98 % CE at 150 mA g⁻¹. The reference electrode also suffered from rapid drift in potential. Additives were generally beneficial to the CE of GBL, especially at slower cycling rates. However, there were some exceptions as TTSPI caused lower CE, whereas an unstable behavior was initiated by additive ES.

From ICI we again see that the additive-free electrolyte had a distinct first charge resistance. A key feature during the first charge was a pronounced double resistance peak (Figure 10).

In GBL, the resistance stabilized later than for PC. Furthermore, the double peak suggests a distinct two-step SEI formation process. Similar to PC, only some of the selected additives alter the characteristic behavior of the resistance profile. ES, FEC, PES, and VC altered the resistance profile to a single resistance peak. These subsequently stabilized to lower resistances than what was obtained for neat GBL. The cell with NaBOB showed a double peak, albeit modified. The distance between the peaks was narrower and the final resistance was lower. TTSPI again showed dissimilar behavior to the rest of the GBL formulations. The initially low resistance increased; by the end of the charge, the anode resistance was higher compared to that in the cell with neat GBL. A trend of decreasing resistance with cycling was generally observed for GBL. Figures 10b and 10c show that the resistance in both additive-free GBL and GBL containing ES decreased with cycling, whereas the well performing additive formulation GBL-PES generated a low and stable resistance (Figure 10d).

2.1.1.3. γ -Valerolactone (GVL)

GVL is similar to GBL in an analogous way to PC and ethylene carbonate. Although GVL has been investigated for lithium batteries, GVL has not been as appealing as its cousin GBL.^[32,39] An advantage with GVL is that it is obtained from cellulosic biomass and can be considered a “green solvent”.^[40] The liquid temperature window of GVL is respectable, with a freezing and

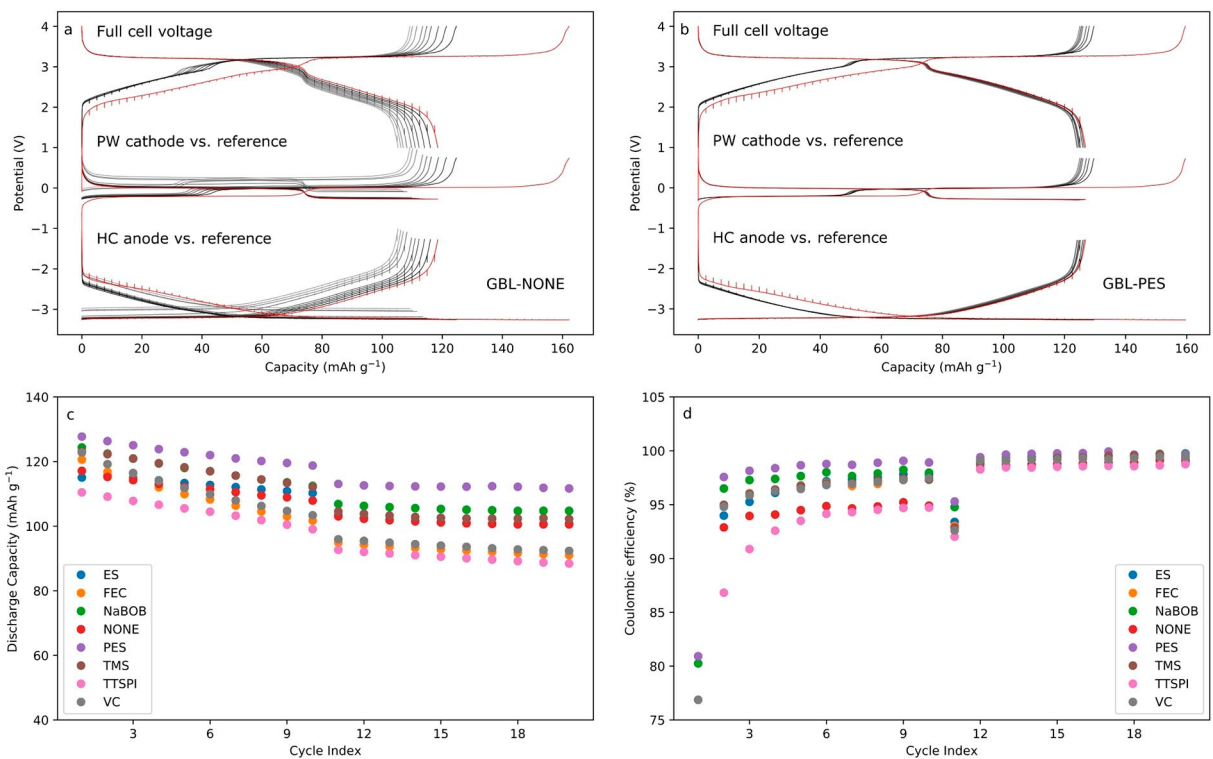


Figure 9. Galvanostatic cycling for ten cycles of three-electrode cells using 1 M NaPF₆ in GBL without additive (a) and with 2 vol% PES (b). Three electrode cells used a PW reference electrode at 3.3 V vs. Na⁺/Na. Discharge capacities (c) and Coulombic efficiency (d) of 1 M NaPF₆ in GBL electrolyte with different additives cycled in two electrode full-cells at 30 mA g⁻¹ for the first ten cycles and 150 mA g⁻¹ for the subsequent ten cycles.

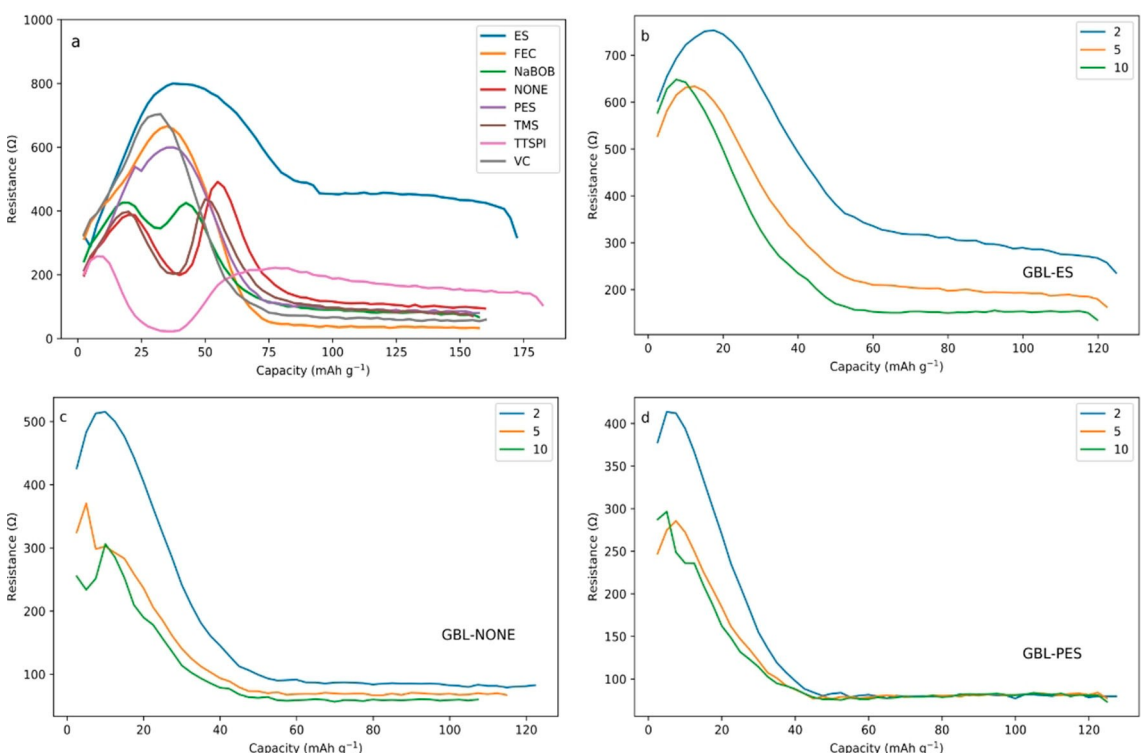


Figure 10. Resistance of the hard-carbon electrode during the 1st charge for all GBL electrolyte formulations (a) with the resistance during 2nd, 5th, and 10th cycle charge for GBL-ES (b), Additive-free GBL(c), and GBL-PES formulations (d).

boiling point of -31°C and 208°C respectively,^[40] while the conductivity is close to 10 mS cm^{-1} at concentrations of 0.94 molal NaPF_6 .

Additive-free GVL electrolyte displayed poor performance (Figure 11): The initial CE average was 53% and the 20th cycle average discharge capacity reached only 52.5 mAh g^{-1} . The ICE in GVL was troublesome in all electrolyte formulations, and the best additive, TTSPI, only raised the average ICE to 58.5%. GVL had moderate capacity fading after the first charge, displaying the same trend as GBL and PC, but with a more substantial capacity fading at slow cycling rates and drifting reference electrodes.

TTSPI, the best performing additive, raised the 20th cycle average discharge capacity from 52.5 mAh g^{-1} to 75.5 mAh g^{-1} . Although the relative improvement in performance was significant, it is apparent that all the additives used for GVL fails to effectively passivate hard-carbon. Nevertheless, the relative improvement of GVL based electrolytes by TTSPI additive, means that there is still hope that this green solvent can be tamed if the right additive is used.

Since GVL showed unstable behavior in the galvanostatic cycling, it is not surprising that the resistance profile in the first charge was quite different than the previous solvents. In GVL, only TTSPI and ES differed significantly from the additive-free electrolyte (Figure 12). TTSPI altered the resistance profile of GVL slightly, and this correlated with it being the only additive providing any beneficial passivation. Although the resistance was not significantly lowered as compared to the neat GVL. ES

again showed deviant behavior and detrimental effects in GVL. PES worked well with GBL, however, for GVL a high initial resistance was observed, which increased with cycling.

2.1.1.4. N-Methyl-2-Pyrrolidone (NMP)

NMP is a potent solvent which needs no introduction for battery scientists; it is often used to dissolve PVDF binder in the slurry coating process but is rarely employed as an electrolyte solvent. The widespread use of NMP in industry originates from its outstanding properties as a solvent combined with its low vapor pressure and a wide temperature window; the freezing point being -23°C and boiling point 202°C .^[41] NMP has been investigated for use in lithium-ion batteries. Due to the low vapor pressure and ability to dissolve many polymers, these trials mostly include use in lithium-air systems and gel-electrolytes.^[42-45]

The galvanostatic cycling of additive-free NMP was somewhat successful at low current densities (30 mA g^{-1}). The average ICE reached 70.5%, and the average discharge capacity was 104 mAh g^{-1} at the 10th cycle. However, the additive-free NMP displayed poor cycling performance at higher rates (150 mA g^{-1}). The CE was consistently low and capacity fading was considerable at 30 mA g^{-1} (Figure 13).

The ICE increased for NMP containing FEC, PES, and VC, as these additives achieved 77.9%, 74.3%, 77.9% average ICE, respectively. VC, PES, NaBOB, and FEC all stabilized the cycling of

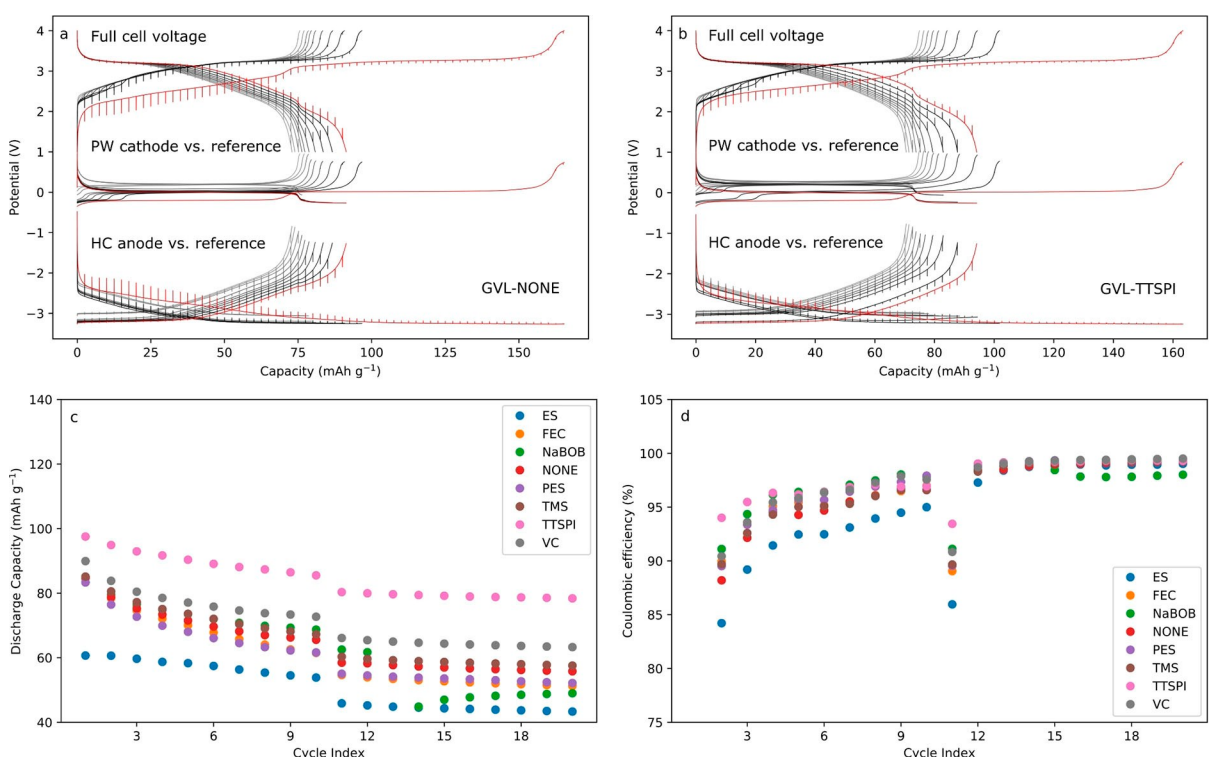


Figure 11. Galvanostatic cycling for ten cycles of three-electrode cells using 1 M NaPF_6 in GVL without additive (a) and with 2 vol % TTSPI (b). Three electrode cells used a PW reference electrode at 3.3 V vs. Na^+/Na . Discharge capacities (c) and Coulombic efficiency (d) of 1 M NaPF_6 in GVL electrolyte with different additives cycled in two electrode full-cells at 30 mA g^{-1} for the first ten cycles and 150 mA g^{-1} for the subsequent ten cycles

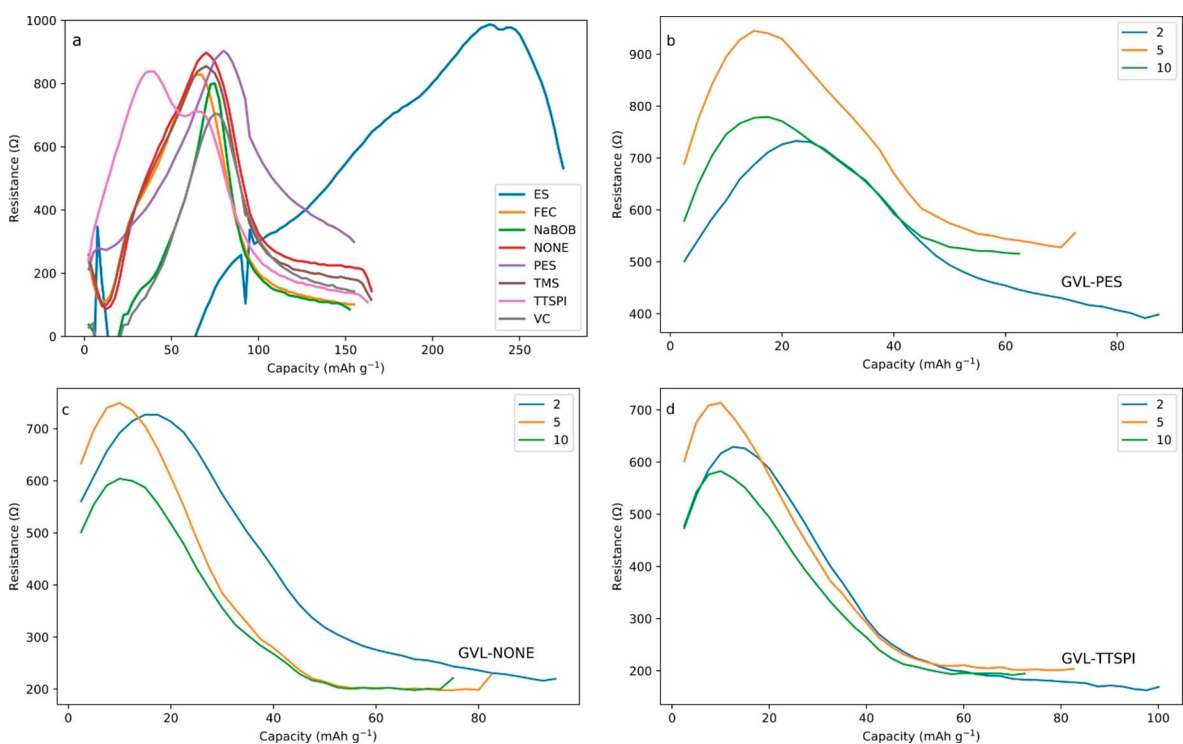


Figure 12. Resistance of the hard-carbon electrode during the 1st charge for all GVL electrolyte formulations (a) with the resistance during 2nd, 5th, and 10th cycle charge for GVL-PES (b), Additive-free GVL (c), and GVL-TTSPI formulations (d).

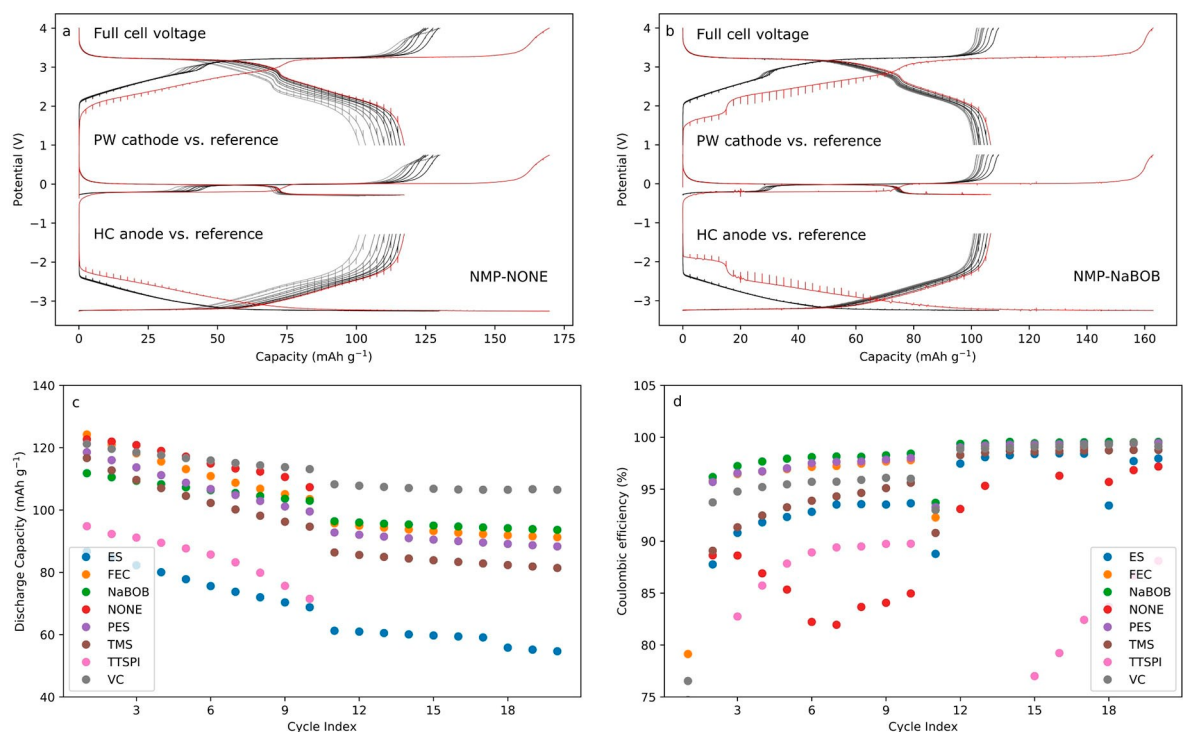


Figure 13. Galvanostatic cycling for ten cycles of three-electrode cells using 1 M NaPF_6 in NMP without additive (a) and with 2 wt% NaBOB (b). Three electrode cells used a PW reference electrode at 3.3 V vs. Na^+/Na . Discharge capacities (c) and Coulombic efficiency (d) of 1 M NaPF_6 in NMP electrolyte with different additives cycled in two electrode full-cells at 30 mA g^{-1} for the first ten cycles and 150 mA g^{-1} for the subsequent ten cycles.

NMP and the CE started from 95% at the second cycle and showed an increasing trend. Additionally, all the previously mentioned

additives showed improved CE at an increased cycling rate (150 mA g^{-1}), while the energy efficiency ranged from 90–95%.

It is clear that the choice of additive has a large impact on the cycling stability of NMP. The impact of additives is clearly visible in the voltage profile close to 4 V during charge, where side reactions were efficiently suppressed by NaBOB and VC (Figures 13a and 13b). VC additive provided the best 20th cycle average discharge capacity at 98 mAh g⁻¹, while FEC (78.3 mAh g⁻¹) and NaBOB (88.5 mAh g⁻¹) also enabled more stable cycling. Still, the overall performance was inferior to GBL and PC. Moreover, the variability in the NMP systems was significant (see Table S8).

The first charge resistance profiles of the anode in NMP-based electrolytes mixed with FEC, TMS, and VC were somewhat similar to the additive-free electrolyte. In contrast, NaBOB, PES, and ES all increased the resistance. Yet, NaBOB stood out, as cycling with additive NaBOB displayed a stable resistance over time (Figure 14). TTSPI and ES were polar opposites with regards to the resistance profiles, but both were detrimental to cell stability. NMP seemed to have one of the lowest overall resistances of the solvents used in this work, and this will be further explored in the case of binary electrolytes.

2.1.1.5. Trimethyl Phosphate (TMP)

TMP is commonly used as a fire-suppressing additive in several applications including batteries.^[46–50] TMP has an attractive combination of properties: The low freezing point (-46°C) makes it promising for low temperature applications. Conversely, the non-flammable attributes and high boiling point

(197°C) also makes it attractive for high temperature applications. In addition, TMP is a cheap solvent, but a major drawback is its incompatibility with hard-carbon unless high salt concentrations or additives are used.^[51]

In cycling voltammetry, the stability of TMP was promising and rivaled that of PC. However, as expected, the additive-free TMP cells were unstable against hard-carbon, where the average ICE was 42.3% and 20th cycle average discharge capacity was 20.5 mAh g⁻¹.

NaBOB and VC showed good compatibility with TMP; the average ICE was improved to 67.5% when using VC. Furthermore, the CE quickly reached values above 95% at 30 mAh g⁻¹ when NaBOB or VC was present in the electrolyte. TMP mixed with NaBOB or VC was capable of cycling at 150 mAh g⁻¹ and the best capacity retention at the 20th cycle for TMP-VC was 85 mAh g⁻¹ (Figure 15).

The initial charge resistance profiles for TMP can be divided into three different cases: 1) The functional additives VC, FEC, and NaBOB, that displayed one initial resistance peak that progressed to a stable low resistance at end of the first charge. 2) Additive-free TMP and TMP-TMS that both showed a double peak resistance profile which never fully stabilized and displayed intermediate resistance. 3) TTSPI and ES that delayed a resistance increase, with subsequent high resistances at the end of the charge. As cycling progresses, well performing additives such as VC showed a low and quite stable resistance. In contrast, additives like PES with mediocre cycling performance showed an overall high resistance, which was almost six

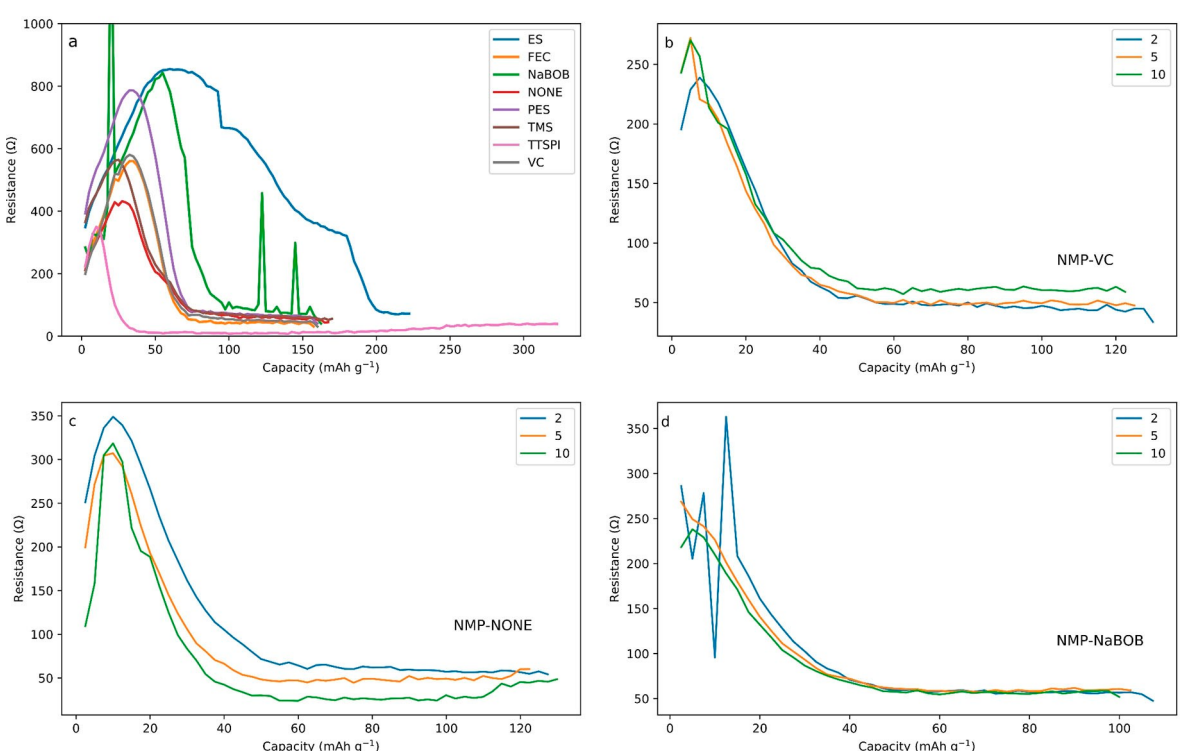


Figure 14. Resistance of the hard-carbon electrode during the 1st charge for all NMP electrolyte formulations (a) with the resistance during 2nd, 5th, and 10th cycle charge for NMP-VC (b), Additive-free NMP (c), and NaBOB-NMP formulations (d).

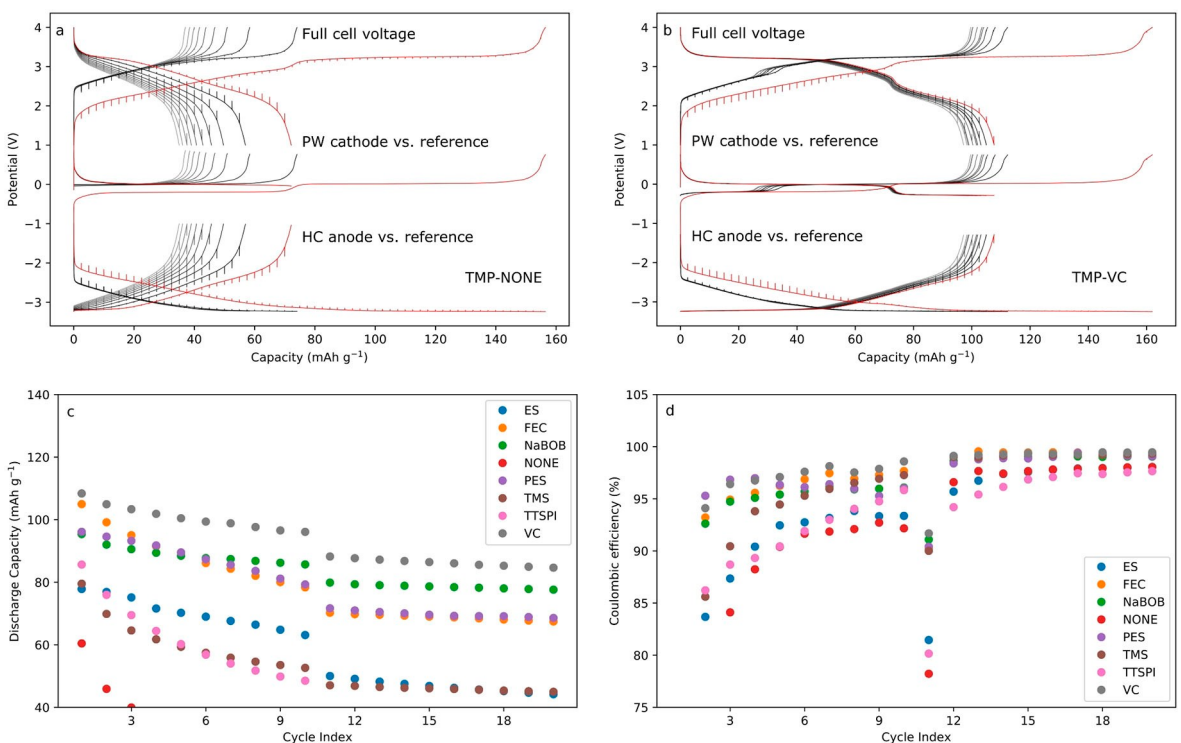


Figure 15. Galvanostatic cycling for ten cycles of three-electrode cells using 1 M NaPF_6 in TMP without additive (a) and with 2 vol % VC (b). Three electrode cells used a PW reference electrode at 3.3 V vs. Na^+/Na . Discharge capacities (c) and Coulombic efficiency (d) of 1 M NaPF_6 in TMP electrolyte with different additives cycled in two electrode full-cells at 30 mA g⁻¹ for the first ten cycles and 150 mA g⁻¹ for the subsequent ten cycles.

times higher than what was obtained when using VC (Figure 16).

2.1.1.6. Sulfolane Mixtures

TMS is a cheap solvent that has found frequent use in the petrochemical industry. It provides good solvent properties and excellent high temperature performance, but is solid at room temperature. It is possible to lower the melting point of TMS by adding salts.^[52] Yet, the high melting point means that TMS, just like ethylene carbonate is not practical as a single solvent. However, the results from our initial trials, and previous works by other authors, attest that TMS is a promising electrolyte solvent.^[53-56] In our study, the cells with additive-free TMS displayed an ICE of 64–67%, with energy efficiencies close to 90% when cycling at 30 mA g⁻¹. The most common measure to rectify the high melting point of TMS is to use it in combination with co-solvents. This is done to boost the ionic conductivity and low temperature performance. As such, TMS was tested in 1:1 mixtures with NMP, DME, TMP and MA, all containing 1 M NaPF_6 . The TMS mixtures with NMP and DME provided stellar performance, whereas the mixture with TMP resulted in a mediocre performance (Figure 17). It should be noted that the three-electrode cells using TMS-TMP electrolyte dramatically outperformed the two-electrode cell counterparts, and we attribute this to the stack pressure that was applied to these cells. MA was tested as a co-solvent due to its low viscosity and high ionic conductivity, but unfortunately the mixture proved

completely non-functional as an electrolyte. The binary mixtures of TMS with NMP and DME were among the best performers out of all the tested electrolytes. Here the average ICE was 80.8% and 82.2% and the 20th cycle average discharge capacities was 119.5 and 121 mA g⁻¹ for TMS-NMP and TMS DME respectively. The results reaffirm that mixing solvents can be as good as, or even better than, using additives in single solvents. Combining both strategies is of course a tempting proposition.

The anode resistance for the electrolytes based on TMS-DME and TMS-NMP disclosed stable behaviors. However, TMS-TMP was more dysfunctional (Figure 18). It is intuitive that the low anode resistance is beneficial for TMS-NMP and TMS-DME electrolytes. Yet, it is unlikely that the anode resistance alone is the cause of suboptimal performance of TMS-TMP. The low current-rates combined with the generously extended cut-off potentials suggests that it was not the resistance causing the poor performance. A more likely failure mechanism would be a depletion of the sodium-inventory. Loss of sodium-inventory would be a consequence of an SEI that is not stable, and the change of the resistance could coincide with unwanted side reactions.

2.1.1.7. TEGDME mixtures

TEGDME or tetraglyme is one of the few solvents that are stable against sodium metal. It has low volatility, low flammability^[57] and an impressive liquid range between -30°C and 275°C .

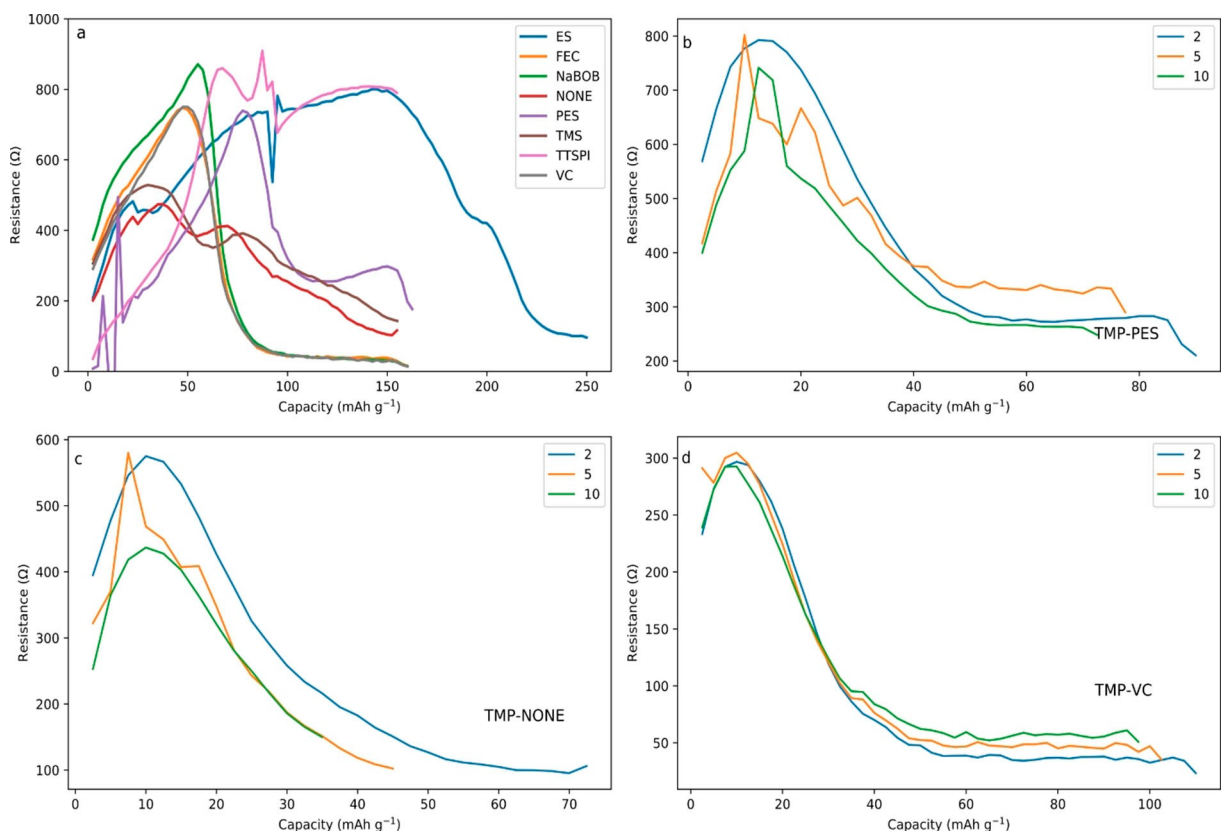


Figure 16. Resistance of the hard carbon electrode during the 1st charge for all TMP electrolyte formulations (a) with the resistance during 2nd, 5th, and 10th cycle charge for TMP-PES (b), additive-free TMP(c), and TMP-VC formulations (d).

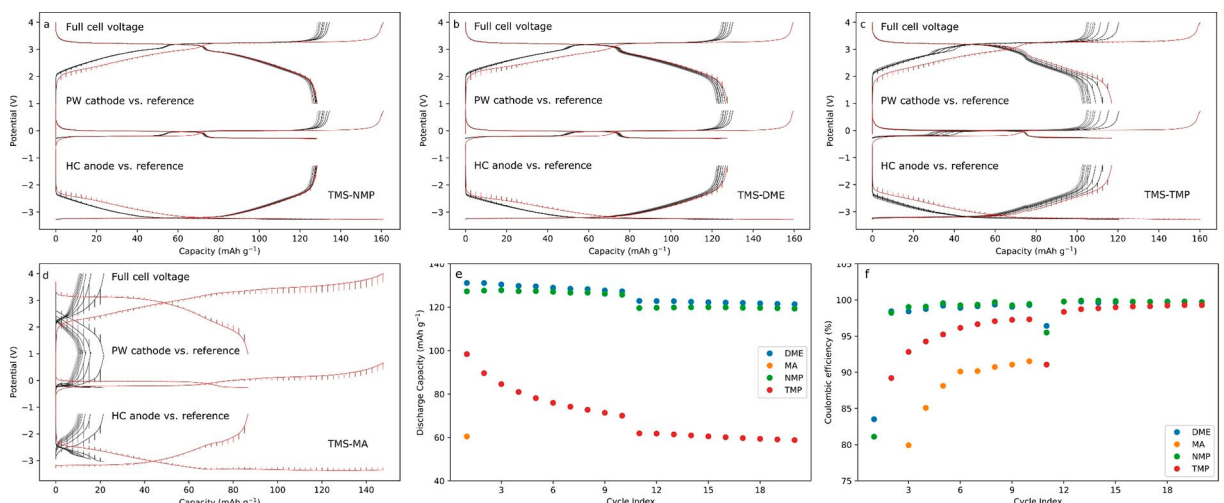


Figure 17. Galvanostatic cycling for ten cycles of three-electrode cells using 1 M NaPF₆ in binary mixture of TMS with 50 vol % NMP (a), DME (b), TMP (c), and MA (d). Three electrode cells used a PW reference electrode at 3.3 V vs. Na⁺/Na. Discharge capacities (e) and Coulombic efficiency (f) for ten cycles in two-electrode full-cells at current density of 30 mA g⁻¹ followed by 10 cycles at 150 mA g⁻¹.

Given these attractive properties, it is no surprise that TEGDME has been considered as an electrolyte solvent in a variety of sodium-ion battery system.^[57–61] During the initial tests, TEGDME achieved ICE values of 67% and the capacity fade was typically less than 20 mAh g⁻¹ after ten cycles in full-cells. Unfortunately, TEGDME had a low ionic conductivity

(2 mS cm⁻¹), which was likely caused by a high viscosity. While TEGDME is in itself a functional solvent from a chemical perspective, it still needs a higher ionic conductivity to be a practical option.

1 M NaPF₆ in TEGDME mixed with NMP, DME, and TMP (1:1 ratio) was prepared and evaluated. Mixtures containing NMP

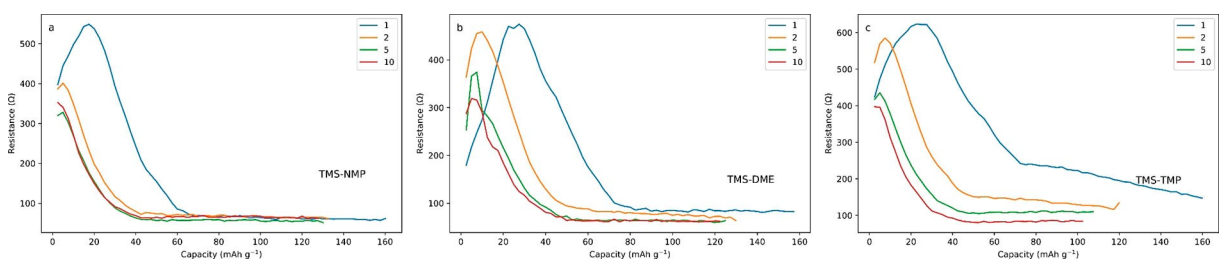


Figure 18. Anode resistance during 2nd, 5th, and 10th cycle charge of Prussian white – hard carbon full-cells using TMS:NMP (a), TMS:DME (b), and TMS:TMP (c) electrolytes.

and DME outperformed the pure TEGDME during the first ten cycles at 30 mA g⁻¹ while the TMP mixture suffered from inconsistent behavior. Cycling at 150 mA g⁻¹, however, led to unstable cycling for all TEGDME mixtures. Here the onset of higher currents caused quick loss of capacity in all cells, regardless of co-solvent (Figure 19).

The resistance evolution of the anodes in TEGDME mixtures generally showed high initial values that increased as cycling progressed (Figure 20). Both DME and NMP mixed with TMS displayed promising performance. This indicates that TEGDME is the main cause for the suboptimal SEI formation when used

either with DME or NMP. For TEGDME-TMP, however, the behavior was different. Here the resistance became lower with each cycle, and this was probably due to the high instability of TMP that led to TMP dominating film formation processes.

2.1.2. Additives

In many cases, the function of an electrolyte additive is uniquely tied to the base solvent. It is thus complicated to discuss each additive in isolation. Nevertheless, in the following

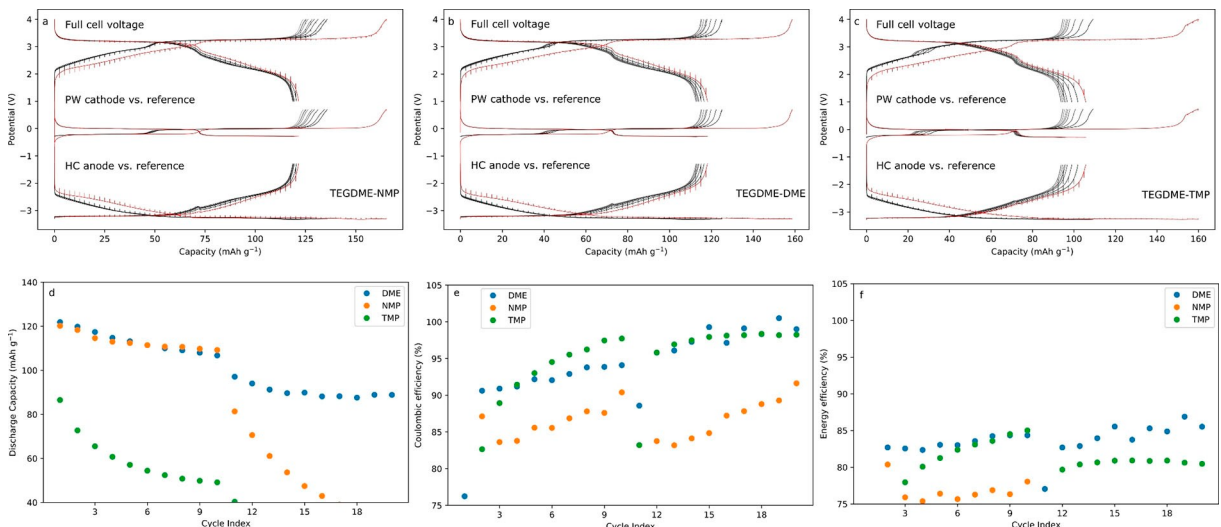


Figure 19. Galvanostatic cycling for ten cycles of three-electrode cells using 1 M NaPF₆ binary mixture of TEGDME with 50 vol % NMP (a), DME (b), and TMP (c). Three electrode cells used a PW reference electrode at 3.3 V vs. Na⁺/Na. Discharge capacities (d), Coulombic efficiency and energy efficiency (e) for ten cycles in two electrode full-cells at 30 mA g⁻¹ followed by ten cycles at 150 mA g⁻¹.

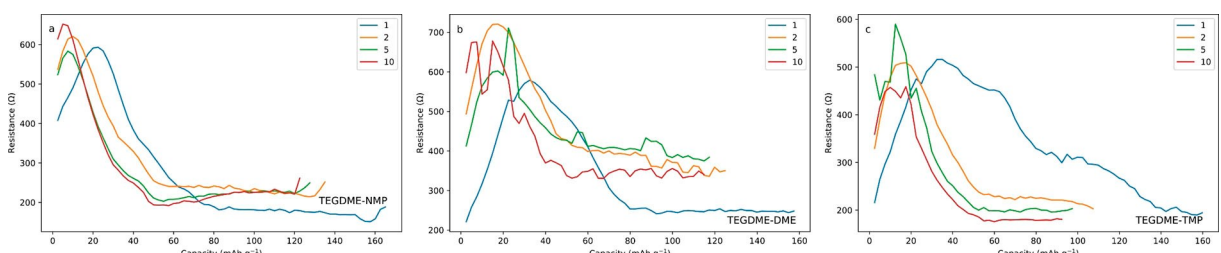


Figure 20. Anode resistance during 2nd, 5th, and 10th cycle charge (red) and discharge (blue) for TEGDME:NMP (a), TEGDME:DME (b), and TEGDME:TMP (c) formulations.

section the general trends of each additive will be presented and discussed. Figure 21 shows a summary of the discharge capacity as well as the anode and cathode resistance during the first charge for solvents used without additives. This figure provides the baseline to which all the different additives are compared.

2.1.2.1. Ethylene Sulfite (ES)

Ethylene sulfite is an organosulfur compound that has been widely used in LIBs to passivate graphite. The poor reduction stability of ES allow for the creation of an SEI before solvents can co-intercalate into graphite; thus enabling the use of solvents like PC.^[62] This compatibility of PC with ES is explained in DFT simulations, where ES was shown to be more reactive than PC and other additives like VC.^[63] Previous studies on

using ES reported negative effects on battery performance in carbonate-based solvents for sodium-ion batteries.^[26,64] Our results indicate that this is true for most other solvents as well. Ethylene sulfite delivered poor ICE in most solvents. Furthermore, ES did not show any significant beneficial effects on capacity retention. In fact, PC and GBL were the only solvents where ES was not detrimental to the cycling (Figure 22a). We observed no indications from ICI that ES was active at the cathode (Figure 22b) but as expected, it influenced the resistance behavior of the anode in all tested solvents.

Additives should be reactive, but the poor performance of ES when used with hard carbon seems to originate from the combination of high reactivity with poor SEI formation. This is indicated by the irregular resistances displayed in ES systems. A comparison between all solvents show that the first cycle anode resistance was invariably higher than the control samples (Figure 22c).

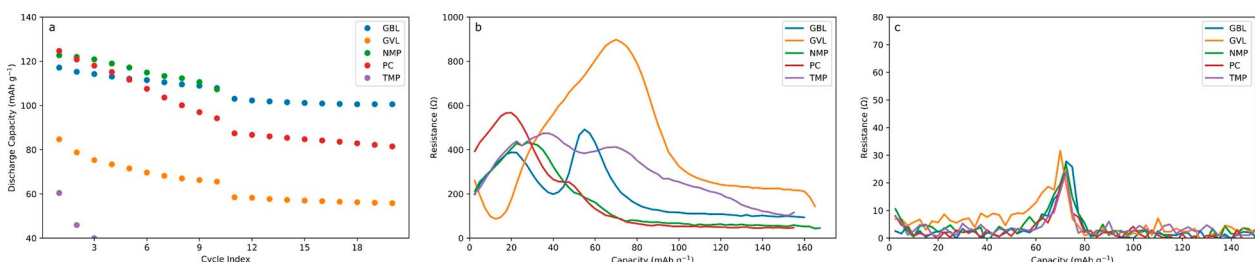


Figure 21. Discharge capacities during ten cycles in two electrode full-cells at 30 mA g⁻¹ followed by ten cycles at 150 mA g⁻¹ (a) and the first charge resistance of the anode (b) and cathode (c) for all additive-free electrolyte formulations.

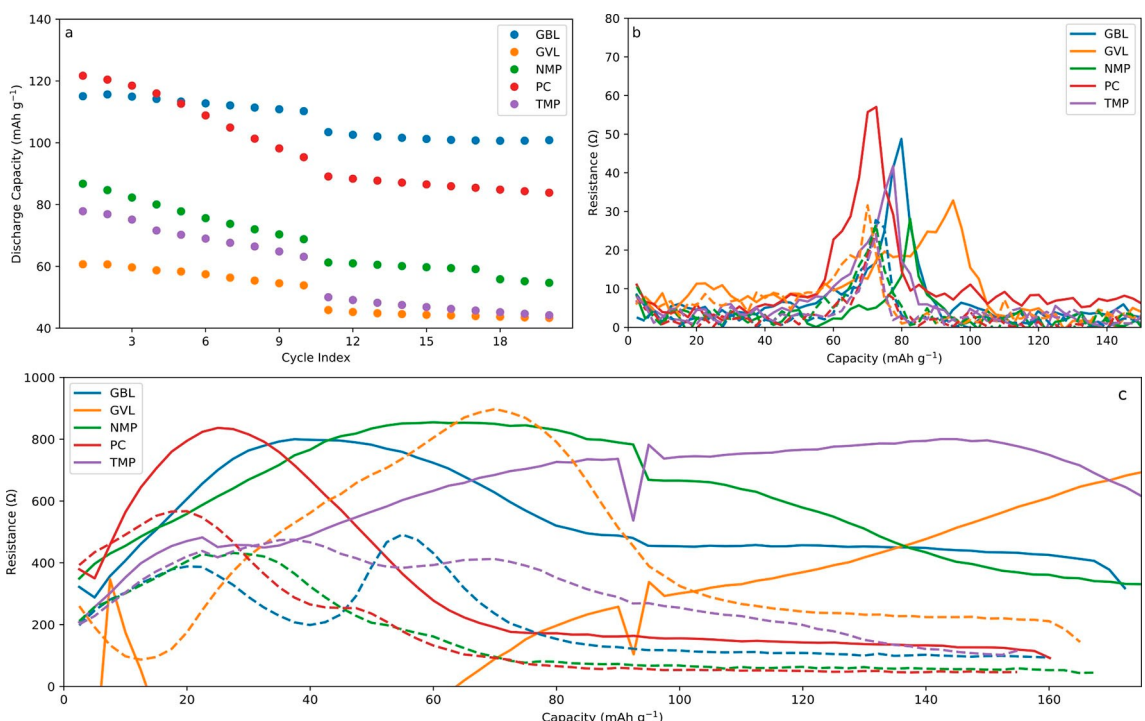


Figure 22. Discharge capacities during ten cycles in two-electrode full-cells cycled at 30 mA g⁻¹ followed by ten cycles at 150 mA g⁻¹ (a) and the first charge resistance of the cathode (b) and hard carbon (c) from all ES containing electrolyte formulations. The solid line indicates solvent with additive while dotted line indicates the same electrolyte without additive

2.1.2.2. Fluoroethylene Carbonate (FEC)

Fluoroethylene carbonate has been widely used in sodium ion batteries, both in hard carbon half-cells and in full-cells. The majority of the literature examines FEC in carbonates^[8,64–69] or TMP.^[51,70–72] It is also usually the first choice of additive to test with any other solvent, since it is very beneficial when sodium metal is present. FEC has been shown to stop decomposition of PC in both half and full-cells.^[26] However, there are some contradictions whether or not it is beneficial to use FEC in hard carbon system since the resistance of the SEI can lower the accessible capacity.^[67] The function of FEC is greatly affected by many factors like additive concentration, binder type, and solvent chemistry. For example, FEC has been shown to be more beneficial when using PVdF binder in the anodes than for NaCMC binder^[65] like the one used in this study. In addition, this study chose 2 vol% based on articles using PC, but in other works using other solvents like TMP the amount can reach as high as 10 vol%.^[72] FEC decomposes at about 0.7 V vs. Na⁺/Na in PC and has been shown to form a mostly inorganic SEI contributing to formation of NaF on the surface layer.^[26] In our study, the decomposition potential of FEC appeared to be high enough to participate in the formation of SEI in all solvents except GVL. Our results from FEC indicate that the additive increases the ICE. In many cases, such as for TMP, this increase was quite dramatic, and was followed by a general improvement in CE in the subsequent cycles for most cells and solvents (Figure 23a).

Capacity retention was most clearly improved for NMP and TMP, whereas GVL, GBL, and PC showed a much smaller improvement during the first twenty cycles. That is, the capacity retention is not significantly improved by FEC in systems that was already quite stable. However, FEC did provide a large improvement to several unstable systems. Yet the effect on GVL was within measurement variations. The reason for this could be a mismatch in decomposition potential as evidenced by the almost unaltered GVL resistance profile during the first charge. This may indicate that decomposition of FEC was absent. Interestingly, TMP showed a slightly increased cathode resistance when FEC was added to the electrolyte. It is however unclear if this was due to the action of TMP or FEC, as TMP shows the propensity to cause such an increase with multiple other additives (see Figure 23b).

If one looks closer at the anode resistance of the first cycle, it is clear that FEC either lowers resistance or matches the pure solvent in the plateau region at the end of charge for all tested solvents (Figure 23c). Overall, the signature of FEC is that it works well in the first cycles but as cycling progresses, or the cycling rate increases, the positive effect is diminished and it is perhaps a bit to reactive in some systems.

2.1.2.3. Sodium Bis(oxalato)borate (NaBOB)

NaBOB is an interesting salt, but it has a limited solubility in most solvents. The BOB⁻ anion appears in LIB literature where LiBOB has been used as both an SEI and CEI former, as well as a

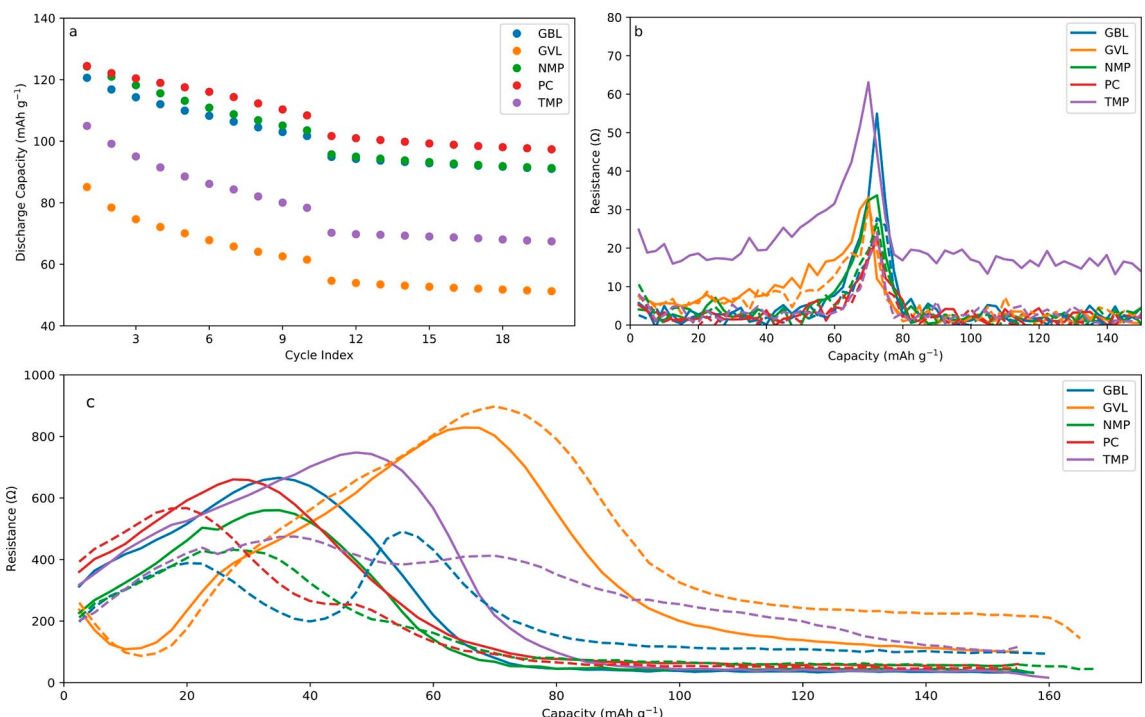


Figure 23. Discharge capacities during ten cycles in two electrode full-cells at 30 mA g⁻¹ followed by ten cycles at 150 mA g⁻¹ (a) and the first charge resistance of the cathode (b) and hard carbon (c) from all FEC containing electrolyte formulations. The solid line indicates solvent with additive while dotted line indicates the same electrolyte without additive.

standalone salt in a wide variety of solvents.^[35,56,73–77] The use of NaBOB in this work is done knowing that the actual concentration in the electrolytes varies significantly between the solvents. The 2 wt% mentioned is the amount of NaBOB added, not necessarily the dissolved amount.

The breakdown of NaBOB was observed in some solvents, like TMP and NMP where the voltage profiles of hard-carbon showed a reduction plateau that appeared at roughly 0.9 V vs. Na^+/Na . The introduction of NaBOB increased ICE for GBL, TMP, and perhaps PC, although the effect on PC was so small that it can be considered as experimental variation. In regards to the capacity retention, there was no difference detected for GBL and GVL. Still, NMP, TMP, and PC all showed better capacity retention with additive NaBOB (Figure 24a). The cathode resistance was slightly elevated for both TMP and GVL when using NaBOB (Figure 24b). However, no action on the cathode was detected in other solvents, with one exception. The cell which used NMP with additive NaBOB displayed an erratic resistance on the first cycle on both the anode and cathode.

In the initial charge ICI results is shown in Figure 24c. The effect of NaBOB is hard to detect in solvents where it has low solubility. Yet, the addition of NaBOB resulted in a lower resistance in TMP and higher resistance in NMP. NaBOB seems to be able to passivate some of the more unstable solvents where it has good solubility like TMP and NMP. For NMP and TMP the passivation comes at the cost of the sodium inventory in the form of low ICE, and the benefits of NaBOB would be augmented if it was mixed with other additives like VC that can help to passivate the electrode during the first charge.^[78]

2.1.2.4. Prop-1-ene-1,3-sultone (PES)

Prop-1-ene-1,3-sultone is in the same category of additives as TMS and ES. PES has likewise been used to successfully hinder PC co-intercalation in graphite.^[79] In the literature, PES is shown to have both SEI (anode) and CEI (cathode) forming properties when used with carbonates in lithium-ion batteries^[80,81] and is regularly used as part of an additive “cocktail”.^[82] PES has also been successfully used in sodium-ion batteries using hard carbon anodes, as part of an additive mix containing FEC, PES, and 1,3,2- Dioxathiolane-2,2-dioxide (DTD).^[83] Given earlier reports, it was no surprise that the most positive results were obtained using PC as the solvent. In other solvents, there were varying degrees of benefits; PES improved ICE considerably in GBL, slightly in NMP and TMP, while leaving ICE in PC mostly unaffected. Within 20 cycles, all the solvents containing PES were superior to their additive free counterparts. PES appears beneficial for both stable and unstable solvents alike, although it did increase the anode resistance in GVL (Figure 25a). There was no firm evidence from resistance measurements that indicate that PES was active at the cathode in the Prussian white – hard carbon system. This might be due to the low upper cut-off voltage compared to many lithium systems (Figure 25b).

The anode resistance of the initial charge reveals that PES interfered with the SEI formation in all solvents except GVL, where the profile closely resembles the additive free solvent (Figure 25c). PES appears to be a semi reactive SEI former, but well-balanced and beneficial for most solvents. Nevertheless, the addition of PES generated an increased resistance com-

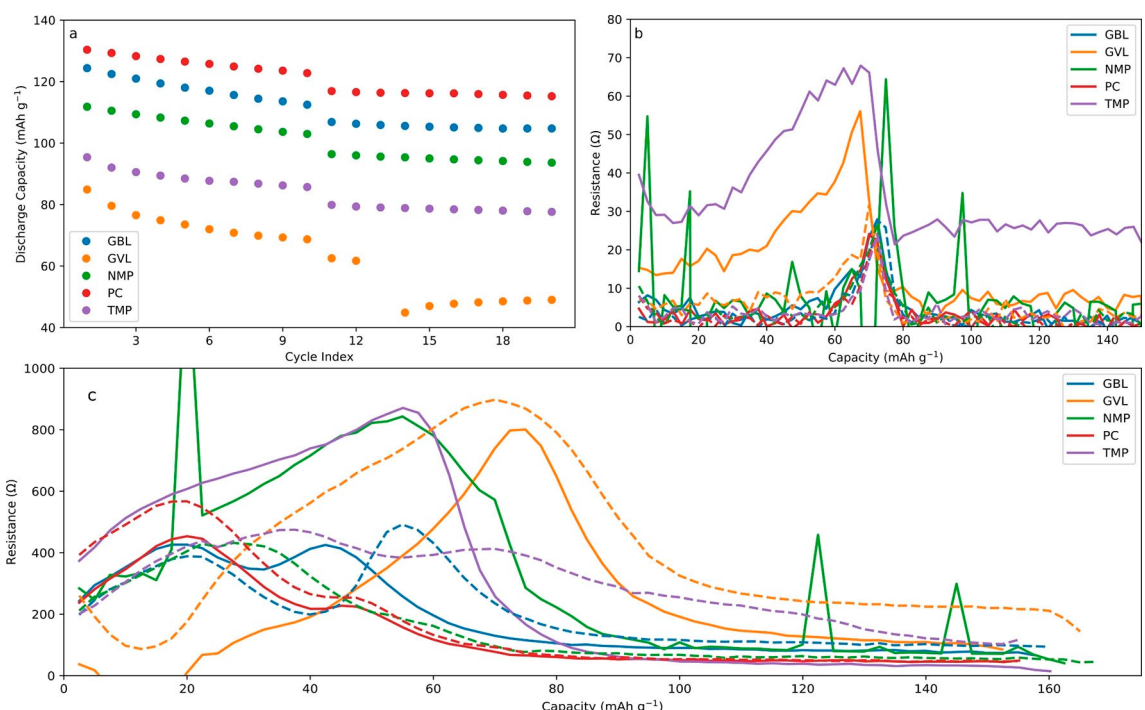


Figure 24. Discharge capacities during ten cycles in two electrode full-cells at 30 mA g⁻¹ followed by ten cycles at 150 mA g⁻¹ (a) and the first charge resistance of the cathode (b) and hard carbon (c) from all NaBOB containing electrolyte formulations. The solid line indicates solvent with additive while dotted line indicates the same electrolyte without additive.

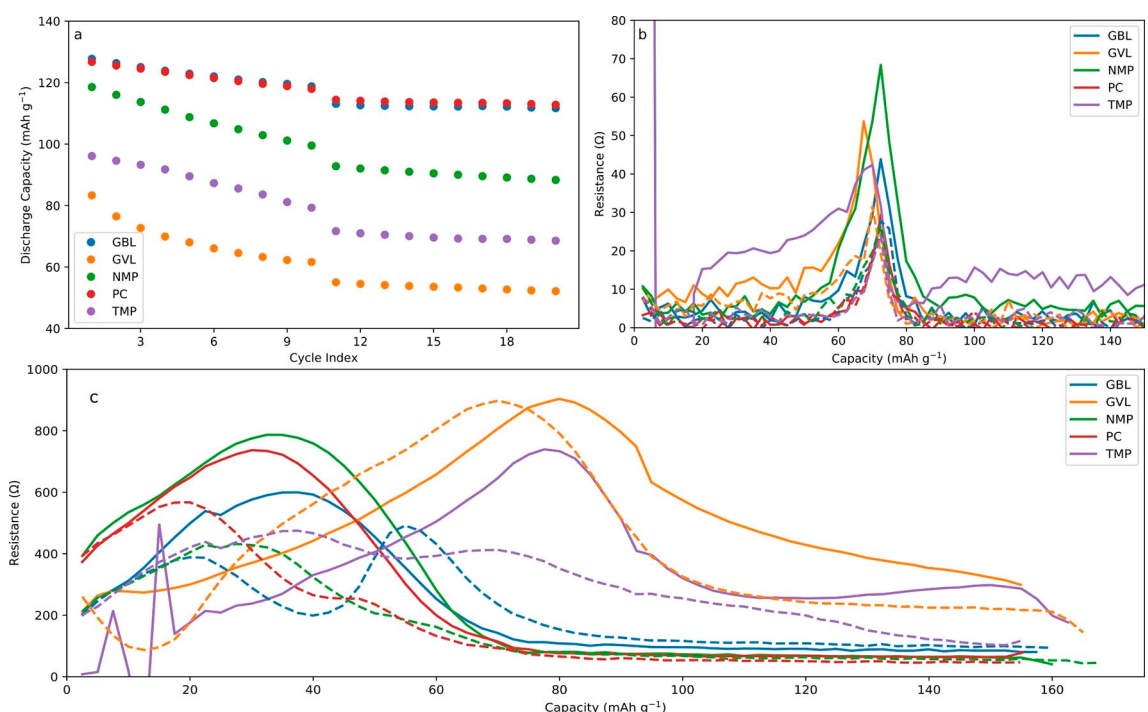


Figure 25. Discharge capacities during ten cycles in two electrode full-cells at 30 mA g⁻¹ followed by ten cycles at 150 mA g⁻¹ (a) and the first charge resistance of the cathode (b) and hard carbon (c) from all PES containing electrolyte formulations. The solid line indicates solvent with additive while dotted line indicates the same electrolyte without additive.

pared to the baseline of most solvents except GBL. This could suggest that the amount of 2% might be higher than what is optimal.

2.1.2.5. Sulfolane (TMS)

The high melting point of TMS can be circumvented by using it as an electrolyte additive. TMS has been reported as an effective additive for graphite-NMC cells in lithium ion battery systems. In these systems, it participates in the SEI formation while also increasing the oxidation stability of the electrolyte.^[84] TMS can be viewed as a less reactive cousin of PES; it is thus expected to have a more limited impact on the cell cycling. The relatively stable nature of TMS was confirmed by the results in our work. Which is in part indicated by TMS's limited influence on ICE values. Still, there were small long-term benefits in certain systems, like PC and GBL. Here, the addition of TMS benefited the capacity retention, although the improvement was small-likely due to the short cycling protocol. In NMP, the increase in CE was especially significant; TMS enabled NMP to function significantly better at higher currents than the reference NMP electrolyte (Figure 26a).

The low reactivity of TMS was confirmed by the ICI measurements of anodes during the first charge (Figure 26c). The signature peaks of each respective solvent was almost identical to the additive-free counterpart when mixed with 5 vol% TMS. In conclusion, TMS seems more suited as a co-solvent than an additive due to its relatively low reactivity; the

binary mixtures of TMS with NMP or DME were both well performing electrolytes.

2.1.2.6. Tris(trimethylsilyl) Phosphite (TTSPI)

TTSPI is an organophosphorus compound and stands out amongst the additives as it contains both phosphorous and silicon. It has been used in lithium-ion batteries, where it has been reported to lower cell impedance in lithium-ion batteries with graphite anodes and NMC cathodes.^[81,85] Again as with PES and TMS, TTSPI is mostly utilized as part of an additive mix with 1–3 additional additives such as VC, DTD, and PES. The effects are reported to include reducing parasitic reactions, lowered gas evolution, and improved high temperature stability.^[86–89] There is little information about the impact of TTSPI on sodium-ion batteries. Our results vary greatly between the different solvents. The effect of TTSPI on ICE does not follow a consistent trend, in PC, the ICE was almost unaffected, for GVL and TMP there was a clear increase. Yet, the additive had a detrimental impact on the ICE for GBL and NMP. The effect of TTSPI as an additive in regards to capacity retention also varied between solvents. GVL and PC responded positively to TTSPI, however, GBL suffers somewhat lowered capacity retention, while NMP showed severe detrimental effects from TTSPI addition (Figure 27a).

A lowered impedance due to the use of TTSPI has been shown by other authors,^[86] this was also generally observed in the ICI results. In solvents where TTSPI improved the cycling, the anode resistance was lower during the initial charge. For

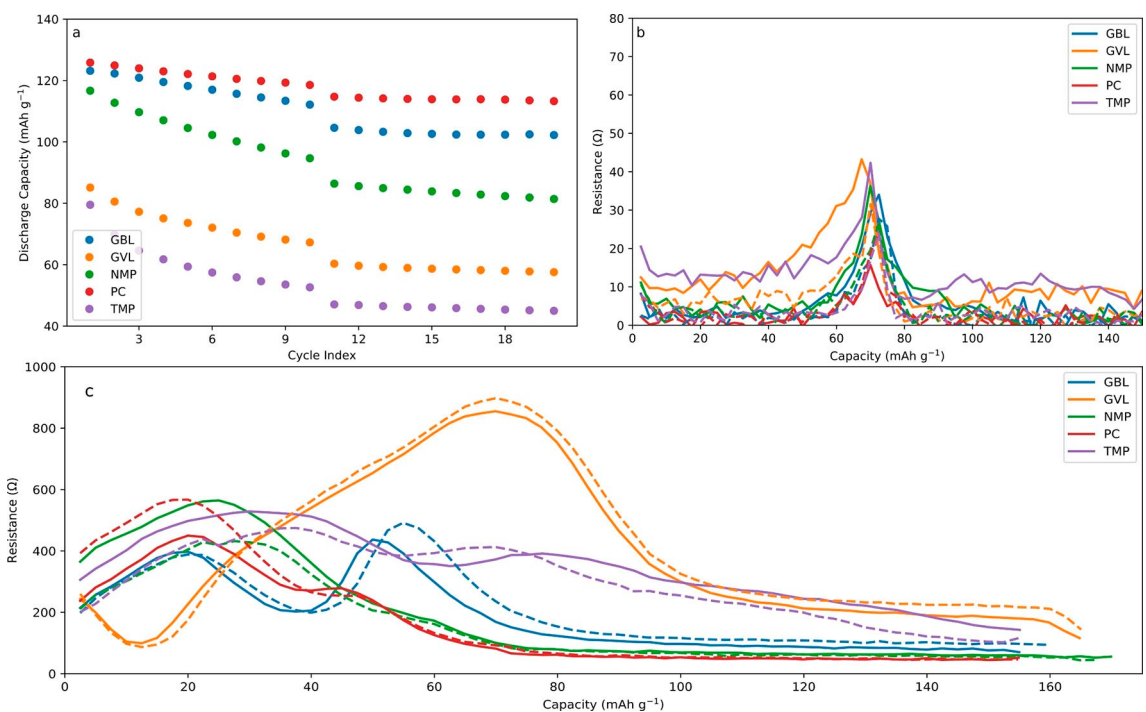


Figure 26. Discharge capacities during ten cycles in two electrode full-cells at 30 mA g⁻¹ followed by ten cycles at 150 mA g⁻¹ (a) and the first charge resistance of the cathode (b) and hard carbon (c) from all TMS containing electrolyte formulations. The solid line indicates solvent with additive while dotted line indicates the same electrolyte without additive.

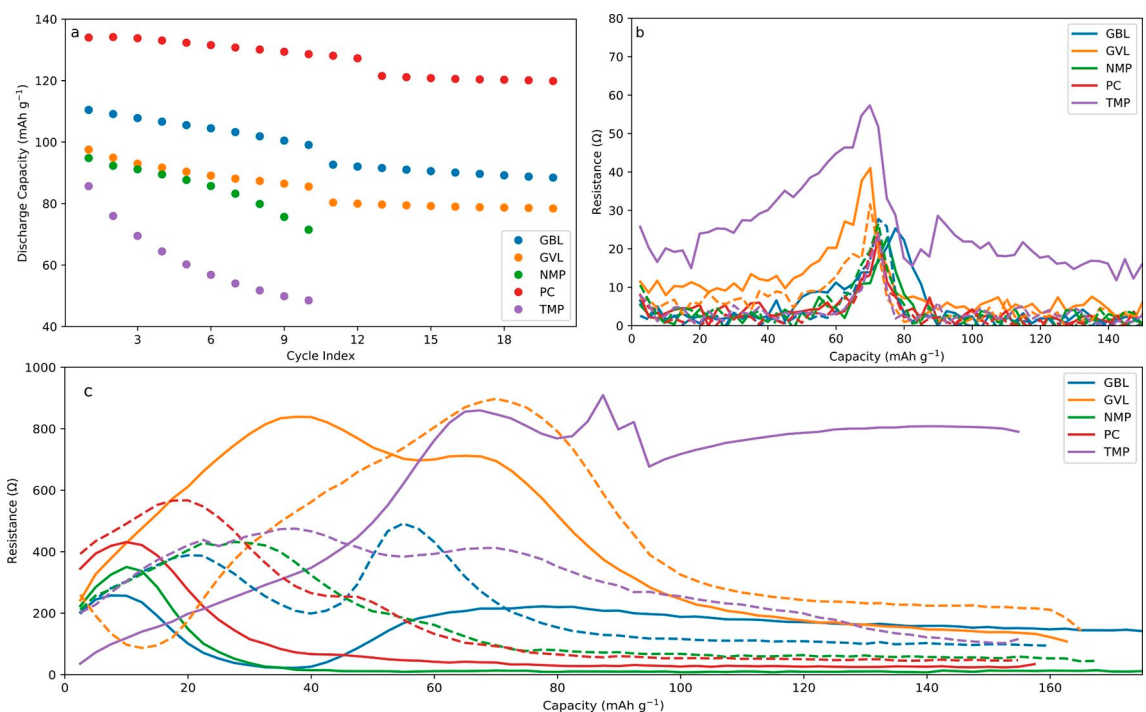


Figure 27. Discharge capacities during ten cycles in two electrode full-cells at 30 mA g⁻¹ followed by ten cycles at 150 mA g⁻¹ (a) and the first charge resistance of the cathode (b) and hard carbon (c) from all TTSPI containing electrolyte formulations. The solid line indicates solvent with additive while dotted line indicates the same electrolyte without additive.

GBL the addition gave an adverse effect on performance. It is noteworthy that the resistance displays a curious and sudden increase during the first charge (Figure 27c). As mentioned

earlier, TTSPI was detrimental for the cell chemistry of NMP and TMP, the effect on resistance was quite interesting. NMP mixed with TTSPI got a remarkably low resistance, whereas TMP

obtains a very high resistance. Regardless of the opposite, extreme resistances, both combinations lead to dysfunctional cells.

2.1.2.7. Vinylene Carbonate (VC)

Vinyl carbonate has been used for a long time. It has proven itself one of the most effective additives in lithium ion batteries; VC together with FEC, is the additive to which all others are compared.^[88,90–93] Whereas FEC has been very popular in sodium-ion batteries, VC has had mixed reviews, and is rarely used. In some systems and articles, VC was reported to have limited – or even a detrimental impact on cycling. This has mostly been shown to be the case for hard-carbon systems.^[26] VC has, however, been shown to perform on par with FEC in systems using phosphorous anodes.^[94] Merely mediocre results might have been expected from VC as an additive, since our study use a hard carbon system. On the contrary, the results tell an entirely different story.

VC showed no measurable effect on ICE for GVL, whereas PC and GBL obtained slight increases. For NMP and TMP the increase in ICE was substantial. Furthermore, the capacity retention was increased for all solvents, except GVL and GBL. Yet, these two did not suffer any significant detrimental effects upon the addition of VC (Figure 28a).

The anode resistance profiles collected during the first charge (Figure 28c) show that VC influenced the formation process in all systems. Quite subtly in GVL. Dramatically, for TMP and GBL. In TMP, VC effectively stabilized the resistance

values to a great extent, indicating promise for long term cycling, even at higher rates. VC would be the clear winner in an overall evaluation of the additives used in our work. In fact, the use of VC in sodium-ion batteries is bound to increase.

3. General Overview

The three-electrode measurements showed that some of the electrolyte systems suffered from drifting reference potential. This was evidenced by the synchronized, symmetric displacement of the anode and cathode voltages during cycling. The drift was consistently to higher potentials. One likely explanation is that the PW reference-electrode was spontaneously sodiated by reactive species produced at the anode, resulting in a drop in the potential. Our hypothesis is thus that the drift was caused by crosstalk between the anode and the reference electrode, which would also mean that the cathode would be spontaneously sodiated as shown in some previous works as well.^[95,96] Unfortunately, inadequate control of the size and mass of the small pieces of reference electrodes made quantification impossible. We refrain from any conclusions until a more focused study has been conducted. Still, it is possible that the self-discharge was quite significant in the systems prone to reference-electrode drift. Some of the electrolytes could cycle over 200 cycles without drift, while other systems showed drift within less than ten cycles (Figure 29). This indicates that whatever caused the drift was electrolyte dependent.

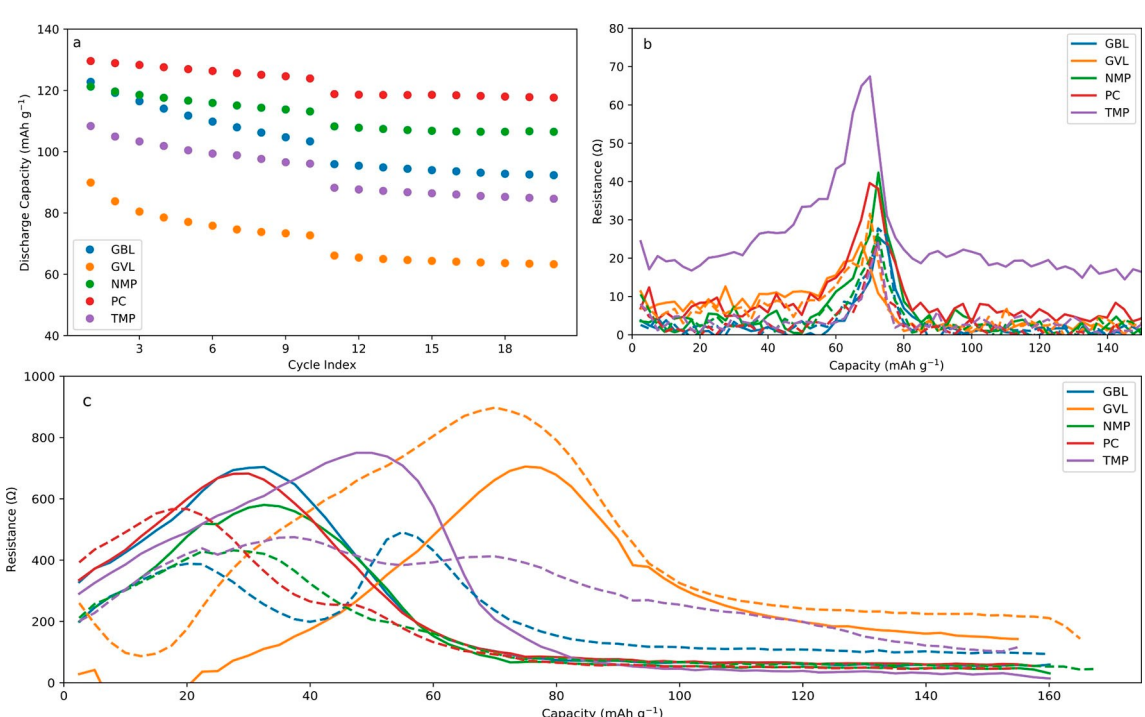


Figure 28. Discharge capacities during ten cycles in two electrode full-cells at 30 mA g^{-1} followed by ten cycles at 150 mA g^{-1} (a) and the first charge resistance of the cathode (b) and hard carbon (c) from all VC containing electrolyte formulations. The solid line indicates solvent with additive while dotted line indicates the same electrolyte without additive.

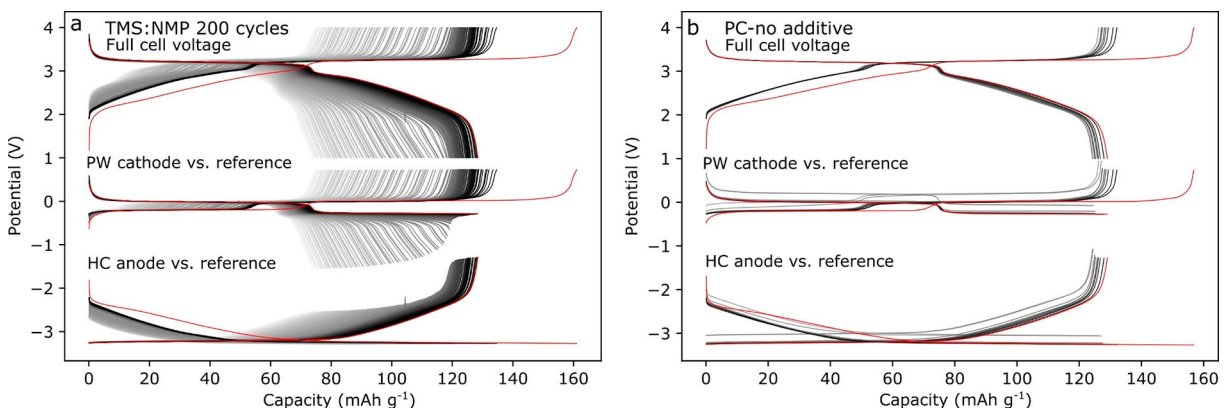


Figure 29. Voltage profiles from Prussian white – hard-carbon three-electrode cells with 200 cycles using 1 M NaPF₆ in TMS:NMP (1:1) electrolyte (a) and ten cycles for 1 M NaPF₆ in PC electrolyte (b), illustrating the drift of the reference electrode in the PC system.

A proper reference electrode needs to have a stable potential. The issue of crosstalk is problematic in this regard. However, insertion-based reference electrodes could possibly be used as redox shuttling probes. If constructed with precision, these probes could elucidate this important parameter in electrolyte and additive studies.

We would like to comment that the ICI measurements were done over a one second time-span, and the drifting electrode should thus not change the results of these measurements. Furthermore, the cut-off potentials were based on the voltage between the anode and cathode, which is unaffected by the reference in the three-electrode cells. The ICI technique can provide information about the stability and resistance of the deposits that form both on the anode and the cathode. Of course, electrochemical impedance spectroscopy (EIS) can give the same information and more, but it is a technique that requires more of the experimental setup. Yet, the ICI technique is robust and can be easily implemented in ordinary three and two-electrode cells. The main practical advantage of ICI is the minimal disturbance to the cell as the short pauses extends the cycling time less than 1% with data points spaced 5 minutes apart. This enables a resistance profile to be recorded with ease whereas the use of EIS in a similar manner would mean prohibitive measurement times.

During the course of this work we found that there are additives that will work as “stand-alone” SEI formers and that there are additives that should be regarded as complementary. Good examples of “stand-alone” SEI formers are NaBOB, FEC and VC. In contrast, TTSPI and TMS are examples of complementary additives that only generate significant improvements if added to relatively stable systems.

Most if not all commercial electrolytes utilize binary or ternary solvent systems. What will work or not in such mixtures is quite hard to predict and there are many mixtures left to explore. Since this strategy is one of the few ways to address poor physical properties of otherwise effective solvents, we encourage the SIB community to widen their candidate pool beyond the classic carbonates and ethers.

We of course recognize that many factors are left unexplored in this study, such as gas evolution, rate capability,

temperature tolerance etc. In this work, our focus is to show that many different electrolyte alternatives are available for sodium-ion batteries, and that each solvent needs different additives to achieve its true potential. What is effective for one solvent can be detrimental for even closely related solvents. It would have been ideal to vary the additive concentrations since this parameter in particular have been shown to be very important in other works.

4. Conclusions

We have investigated several electrolytes consisting of different classes of non-aqueous solvents and NaPF₆ salt. An attempt was made to improve some of the selected electrolytes by using electrolyte additives or binary solvent mixtures. Carbonates, here represented by PC shows excellent performance that can be further augmented by choosing the right additives. However, carbonates are far from the only choice. Several well-functioning alternatives have been presented herein. We have also shown that the ICI technique is a useful and simple tool for electrolyte studies that can provide additional information from galvanostatic cycling. Electrochemical cycling performance in full-cell sodium-ion batteries based on hard-carbon anodes and Prussian white cathodes was the main evaluation criteria. This was needed since metallic sodium was incompatible with many of the tested electrolytes. There are many combinations of solvents and additives in this work that to our knowledge have never been described before. Some of these merit further investigations. This work only scratched the surface of what practical options exist in the field of SIB electrolytes. Our hope is that the results presented here can help others find the best electrolyte for their system. The results also reveal that the community needs to reinvestigate electrolyte species discarded due to their impracticality for LIBs or sodium half-cells. SIBs and sodium metal hold different characteristics than LIBs and metallic lithium. This work reaffirms many results from previous studies, it does however also have some discrepancies with previous literature. Some results are contrary to conventional notions in SIB literature. One example is the stellar performance

of VC additive for PC and many other solvents, even when cycled vs. hard carbon. Untested tenets can cause such misconceptions, which stand in the way of progress. In summary, the SIB infrastructure has matured and many previously investigated solvents and additives deserve a second chance in new and refined systems.

Experimental Section

Electrolyte preparation

All solvents used were dried over freshly activated molecular sieves before use. These solvents were (and were acquired from): DME (BASF), ethyl acetate (Sigma-Aldrich 99.8% anhydrous), trimethyl phosphate (Acros organics 99%), tetraethylene glycol dimethyl ether (Sigma-Aldrich ≥ 99%), methyl acetate (Sigma-Aldrich 99.5% anhydrous), sulfolane (Sigma-Aldrich 99%), ethyl propionate (Sigma-Aldrich 99%), ethyl butyrate (Sigma-Aldrich 99%), γ-butyrolactone (Merck, Selectipur anhydrous), γ-valerolactone (Sigma-Aldrich 99%), methyl propionate (Sigma-Aldrich), *N*-methyl-2-pyrrolidone (Acros Extra Dry ≥ 99.5%), propylene carbonate (Gotion). NaPF₆ salt (Stella 99%) was dried thoroughly under vacuum before use. The following additives were used as received: ethylene sulfite (Sigma-Aldrich ≥ 99%), vinyl carbonate (Gotion), fluoroethylene carbonate (Gotion), prop-1-ene-1,3-sultone (97% Sigma-Aldrich, Manchester organics), tris(trimethylsilyl) phosphite (Sigma-Aldrich > 95.0%). The sodium bis(oxalato)borate was synthesized according to the method described by Zavalij et al.^[97]

All electrolyte preparation and cell construction were performed under argon in a glove-box. Only mixtures that became fully dissolved and produced a clear solution were considered for study. The electrolytes for initial cycling were prepared by mixing NaPF₆ salt and solvent to prepare concentrations of 0.5, 1, and 1.5 M assuming no volume increase due to the salt addition, due to this lack of precision the exact molal (mol kg⁻¹) concentration was instead used for these samples. All electrolytes were freshly prepared for the testing of additives and binary mixtures. The preparation was done by adding the appropriate amount of dried NaPF₆ salt in a volumetric flask and thereafter adding the solvent or solvent mixture in two steps and letting the salt dissolve to achieve an accurate 1 M concentration of NaPF₆. Binary mixtures were prepared by mixing equal volumes in stock solutions before mixing with the salt, while additives were added to the prepared 1 M NaPF₆ solution of the solvent. Ionic conductivity measurements were performed using a Mettler Toledo SevenGo Duo pro pH/ORP/Ion/Conductivity meter SG78 with an InLab 738ISM probe under argon in a glovebox.

Cell construction

Prussian white cathode powder was supplied by Altris AB and coated by using an applicator rod (150 μm slit width) on carbon coated aluminum foil (leclanche EB-012 20 μm). The coatings consisted of Prussian white, C65 (Erachem) carbon additive and Carboxymethyl cellulose binder (Sigma) mixed in 85:10:5 wt%. The slurry was homogenized in a 60 ml zirconia jar with two 20 mm 25.55 g zirconia balls using a retsch PM-4 ball mill at 150 rpm. The mixture was ball milled with appropriate amounts of water (~4.4 g water per gram dry of mass) for 1 h. The commercial hard-carbon consisted of particles with the following attributes: D_{50} size was 1.3 μm, surface area 22 m² g⁻¹, while the density was 0.75 g cm⁻³. The hard carbon was mixed with 5 wt% C65 and ~5.8 g water per gram of dry mass with an identical ball-milling

procedure as the cathode. The slurry was coated on carbon coated aluminum foil in the same way as the cathodes (100 μm slit width on the applicator rod). The coatings were dried at 140 °C under vacuum overnight and subsequently punched out into 13 mm disks. For initial cycling tests the approximate Prussian white mass loading was 1.8 mg cm⁻², while the additive and binary-solvent tests used new coatings with approximately 2 mg cm⁻² mass loading. In both cases hard carbon electrodes were chosen to provide slight overcapacity (1 mg cm⁻²) as compared to the positive electrode to avoid plating sodium. All cells used 20 mm Whatman glass-fiber that were dried using the same procedure as the electrodes before use. For cyclic and linear sweep voltammetry cells, the working electrode consisted of a 13 mm carbon-coated aluminum foil disk, whereas the counter electrode consisted of an oversized disk of metallic sodium. The reference electrodes used in three-electrode cells were prepared from pieces of Prussian white cathode coatings that had been electrochemically desodiated to 3.3 V and washed using dimethyl carbonate. The cells were assembled in pouch cells using aluminum current collectors and vacuum-sealed (2 mBar) under argon. All cells were assembled using 100 μL of their respective electrolyte formulation. All cells were cycled without additional stack-pressure except for three-electrode cells that were clamped softly between two plates.

Electrochemistry

The cyclic voltammetry and linear sweep voltammetry were performed on a Biologic MPG2 potentiostat between 0.001–4.5 V vs. Na⁺/Na at 1 mVs⁻¹. Galvanostatic cycling was performed using the following instruments: LAND CT2001 A battery tester, Arbin BT-2043 battery testing system, Neware BTS4000 galvanostat while three-electrode cells were cycled on a Biologic MPG2 potentiostat. The cut-off potential limits were 4 V and 1 V and the applied current was set to 30 mA g⁻¹ based on the active mass of the cathode for the first 10 cycles. The current was thereafter increased to 150 mA g⁻¹ for subsequent cycles. For the ICl measurements, the cycling program used the same voltage cut-off limits and currents as regular galvanostatic cycling with the exception of 1 s current interruptions at 5 min intervals. During the 1 s current interruption the OCV was sampled with 100 ms intervals to provide the data for resistance calculations.

Acknowledgments:

We would like to thank Dr. Matthew J. Lacey for the scientific discussion. Authors would like to acknowledge the financial support by the ÅForsk Foundation via the grant no. 20-675 and by STandUP for Energy.

Conflict of Interest

The authors declare no conflict of interest.

Keywords: electrolytes • full-cell • hard carbon • Na-ion batteries • solvents

- [1] I. Hasa, S. Mariyappan, D. Saurel, P. Adelhelm, A. Y. Koposov, C. Masquelier, L. Croguennec, M. Casas-Cabanas, *J. Power Sources* **2021**, 482, 228872.

- [2] Q. Liu, Z. Hu, M. Chen, C. Zou, H. Jin, S. Wang, S. L. Chou, Y. Liu, S. X. Dou, *Adv. Funct. Mater.* **2020**, *30*, 1909530.
- [3] Y. Huang, Y. Zheng, X. Li, F. Adams, W. Luo, Y. Huang, L. Hu, *ACS Energy Lett.* **2018**, *3*, 1604.
- [4] K. Xu, *Chem. Rev.* **2014**, *114*, 11503.
- [5] W. A. Henderson, *Electrolytes for Lithium and Lithium-Ion Batteries* (Eds.: Jow, T. R.; Xu, K.; Borodin, O.; Ue, M.), Vol. 58, Springer New York, New York, NY, **2014**.
- [6] J. Song, B. Xiao, Y. Lin, K. Xu, X. Li, *Adv. Energy Mater.* **2018**, *8*, 1703082.
- [7] R. Mogensen, D. Brandell, R. Younesi, *ACS Energy Lett.* **2016**, *1*, 1173.
- [8] G. G. Eshetu, G. A. Elia, M. Armand, M. Forsyth, S. Komaba, T. Rojo, S. Passerini, *Electrolytes and Interphases in Sodium-Based Rechargeable Batteries: Recent Advances and Perspectives*, Vol. 10, **2020**, p. 2000093.
- [9] L. A. Ma, A. J. Naylor, L. Nyholm, R. Younesi, *Angew. Chem. Int. Ed.* **2021**, *60*, 2–11.
- [10] J.-Y. Hwang, S.-T. Myung, Y.-K. Sun, *Chem. Soc. Rev.* **2017**, *46*, 3529.
- [11] H. Pan, Y.-S. Hu, L. Chen, *Energy Environ. Sci.* **2013**, *6*, 2338.
- [12] D. H. Morman, G. A. Harlow, *Anal. Chem.* **1967**, *39*, 1869.
- [13] G. Zeng, S. Xiong, Y. Qian, L. Ci, J. Feng, *J. Electrochem. Soc.* **2019**, *166*, A1217.
- [14] A. Ponrouche, E. Marchante, M. Courty, J.-M. Tarascon, M. R. Palacín, *Energy Environ. Sci.* **2012**, *5*, 8572.
- [15] R. Payne, I. E. Theodorou, *J. Phys. Chem.* **1972**, *76*, 2892.
- [16] H. Lu, J. Wang, Y. Zhao, X. Xuan, K. Zhuo, *J. Chem. Eng. Data* **2001**, *46*, 631.
- [17] N. V. Sastry, S. R. Patel, S. S. Soni, *J. Mol. Liq.* **2013**, *183*, 102.
- [18] G. Moumouzias, C. Ritzoulis, G. Ritzoulis, *J. Chem. Eng. Data* **1999**, *44*, 1187.
- [19] G. Strappaveccia, L. Luciani, E. Bartolini, A. Marrocchi, F. Pizzo, L. Vaccaro, *Green Chem.* **2015**, *17*, 1071.
- [20] J. F. Côté, D. Brouillette, J. E. Desnoyers, J. F. Rouleau, J. M. St-Arnaud, G. Perron, *J. Solution Chem.* **1996**, *25*, 1163.
- [21] J. Wyman, *J. Am. Chem. Soc.* **1936**, *58*, 1482.
- [22] W. R. Brant, R. Mogensen, S. Colbin, D. O. Ojwang, S. Schmid, L. Häggström, T. Ericsson, A. Jaworski, A. J. Pell, R. Younesi, *Chem. Mater.* **2019**, *31*, 7203.
- [23] B. Aktekin, M. J. Lacey, T. Nordh, R. Younesi, C. Tengstedt, W. Zipprich, D. Brandell, K. Edström, *J. Phys. Chem. C* **2018**, *122*, 11234.
- [24] M. J. Lacey, *ChemElectroChem* **2017**, *4*, 1997.
- [25] A. Ponrouche, D. Monti, A. Boschin, B. Steen, P. Johansson, M. R. Palacín, *J. Mater. Chem. A* **2015**, *3*, 22.
- [26] S. Komaba, T. Ishikawa, N. Yabuuchi, W. Murata, A. Ito, Y. Ohsawa, *ACS Appl. Mater. Interfaces* **2011**, *3*, 4165.
- [27] S. Komaba, W. Murata, T. Ishikawa, N. Yabuuchi, T. Ozeki, T. Nakayama, A. Ogata, K. Gotoh, K. Fujiwara, *Adv. Funct. Mater.* **2011**, *21*, 3859.
- [28] M. Carboni, J. Manzi, A. R. Armstrong, J. Billaud, S. Brutti, R. Younesi, *ChemElectroChem* **2019**, *6*, 1745.
- [29] M. Dahbi, N. Yabuuchi, K. Kubota, K. Tokiwa, S. Komaba, *Phys. Chem. Chem. Phys.* **2014**, *16*, 15007.
- [30] L. A. Ma, F. Massel, A. J. Naylor, L.-C. Duda, R. Younesi, *Commun. Chem.* **2019**, *2*, 125.
- [31] M. Moshkovich, Y. Gofer, D. Aurbach, *J. Electrochem. Soc.* **2001**, *148*, E155.
- [32] S. I. Tobishima, T. Okada, *J. Appl. Electrochem.* **1985**, *15*, 317.
- [33] S. C. Kinoshita, M. Kotato, Y. Sakata, M. Ue, Y. Watanabe, H. Morimoto, S. I. Tobishima, *J. Power Sources* **2008**, *183*, 755.
- [34] D. Belov, D. T. Shieh, *J. Solid State Electrochem.* **2012**, *16*, 603.
- [35] P. Shi, S. Fang, J. Huang, D. Luo, L. Yang, S. I. Hirano, *J. Mater. Chem. A* **2017**, *5*, 19982.
- [36] M. L. Lazar, B. L. Lucht, *J. Electrochem. Soc.* **2015**, *162*, A928.
- [37] T. Doi, Y. Shimizu, M. Hashinokuchi, M. Inaba, *ChemElectroChem* **2017**, *4*, 2398.
- [38] V. A. Diamant, S. M. Malovanyy, K. D. Pershina, K. A. Kazdabin, *Mater. Today Proc.* **2019**, *6*, 86.
- [39] M. Vraneš, N. Cvjetićanin, S. Papović, B. Šarac, I. Prislan, P. Megušar, S. Gadžurić, M. Bešter-Rogač, *J. Mol. Liq.* **2017**, *243*, 52.
- [40] D. M. Alonso, S. G. Wettstein, J. A. Dumesic, *Green Chem.* **2013**, *15*, 584.
- [41] A. Jouyban, M. A. A. Fakhree, A. Shayanfar, *J. Pharm. Pharmaceut. Sci.* **2010**, *13*, 524.
- [42] G. T. K. Fey, M. C. Hsieh, H. K. Jaw, T. J. Lee, *J. Power Sources* **1993**, *44*, 673.
- [43] J. Chatterjee, T. Liu, B. Wang, J. P. Zheng, *Solid State Ionics* **2010**, *181*, 531.
- [44] H. Wang, K. Xie, L. Wang, Y. Han, *J. Power Sources* **2012**, *219*, 263.
- [45] S. S. Zhang, K. Xu, T. R. Jow, *Electrochim. Acta* **2006**, *51*, 1636.
- [46] J. Wang, Y. Yamada, K. Sodeyama, E. Watanabe, K. Takada, Y. Tateyama, A. Yamada, *Nat. Energy* **2018**, *3*, 22.
- [47] K. Matsumoto, K. Nakahara, K. Inoue, S. Iwasa, K. Nakano, S. Kaneko, H. Ishikawa, K. Utsugi, R. Yuge, *J. Electrochem. Soc.* **2014**, *161*, A831.
- [48] X. Wang, C. Yamada, H. Naito, G. Segami, K. Kibe, *J. Electrochem. Soc.* **2006**, *153*, 135.
- [49] P. Shi, H. Zheng, X. Liang, Y. Sun, S. Cheng, C. Chen, H. Xiang, *Chem. Commun.* **2018**, *54*, 4453.
- [50] X. L. Yao, S. Xie, C. H. Chen, Q. S. Wang, J. H. Sun, Y. L. Li, S. X. Lu, *J. Power Sources* **2005**, *144*, 170.
- [51] X. Liu, X. Jiang, Z. Zeng, X. Ai, H. Yang, F. Zhong, Y. Xia, Y. Cao, *ACS Appl. Mater. Interfaces* **2018**, *10*, 38141.
- [52] Y. Okamoto, S. Tsuzuki, R. Tatara, K. Ueno, K. Dokko, M. Watanabe, *J. Phys. Chem. C* **2020**, *124*, 4459.
- [53] E. Björklund, M. Göttlinger, K. Edström, R. Younesi, D. Brandell, *Batteries & Supercaps* **2020**, *3*, 201.
- [54] Y. Matsuda, *J. Electrochem. Soc.* **1985**, *132*, 2538.
- [55] S. Li, W. Zhao, X. Cui, Y. Zhao, B. Li, H. Zhang, Y. Li, G. Li, X. Ye, Y. Luo, *Electrochim. Acta* **2013**, *91*, 282.
- [56] L. Mao, B. Li, X. Cui, Y. Zhao, X. Xu, X. Shi, S. Li, F. Li, *Electrochim. Acta* **2012**, *79*, 197.
- [57] A. Rudola, K. Du, P. Balaya, *J. Electrochem. Soc.* **2017**, *164*, A1098.
- [58] I. H. Jo, H. S. Ryu, D. G. Gu, J. S. Park, I. S. Ahn, H. J. Ahn, T. H. Nam, K. W. Kim, *Mater. Res. Bull.* **2014**, *58*, 74.
- [59] H. Ryu, T. Kim, K. Kim, J. H. Ahn, T. Nam, G. Wang, H. J. Ahn, *J. Power Sources* **2011**, *196*, 5186.
- [60] C. Kim, K. Y. Lee, I. Kim, J. Park, G. Cho, K. W. Kim, J. H. Ahn, H. J. Ahn, *J. Power Sources* **2016**, *317*, 153.
- [61] I. Hasa, X. Dou, D. Buchholz, Y. Shao-Horn, J. Hassoun, S. Passerini, B. Scrosati, *J. Power Sources* **2016**, *310*, 26.
- [62] G. H. Wrodnigg, J. O. Besenhard, M. Winter, *J. Electrochem. Soc.* **1999**, *146*, 470.
- [63] M. D. Bhatt, C. O'Dwyer, *J. Electrochem. Soc.* **2014**, *161*, X18.
- [64] M. Dahbi, T. Nakano, N. Yabuuchi, S. Fujimura, K. Chihara, K. Kubota, J. Y. Son, Y. T. Cui, H. Oji, S. Komaba, *ChemElectroChem* **2016**, *3*, 1856.
- [65] M. Dahbi, T. Nakano, N. Yabuuchi, T. Ishikawa, K. Kubota, M. Fukunishi, S. Shibahara, J. Y. Son, Y. T. Cui, H. Oji, S. Komaba, *Electrochim. Commun.* **2014**, *44*, 66.
- [66] Y. Lee, J. Lee, H. Kim, K. Kang, N. S. Choi, *J. Power Sources* **2016**, *320*, 49.
- [67] A. Ponrouche, A. R. Goñi, M. R. Palacín, *Electrochim. Commun.* **2013**, *27*, 85.
- [68] C. Y. Li, J. Patra, C. H. Yang, C. M. Tseng, S. B. Majumder, Q. F. Dong, J. K. Chang, *ACS Sustainable Chem. Eng.* **2017**, *5*, 8269.
- [69] R. Mogensen, J. Maibach, W. R. Brant, D. Brandell, R. Younesi, *Electrochim. Acta* **2017**, *245*, 696.
- [70] J. Wu, J. Liu, Z. Lu, K. Lin, Y. Q. Lyu, B. Li, F. Ciucci, J. K. Kim, *Energy Storage Mater.* **2019**, *23*, 8.
- [71] X. Jiang, Z. Zeng, L. Xiao, X. Ai, H. Yang, Y. Cao, *ACS Appl. Mater. Interfaces* **2017**, *9*, 43733.
- [72] Z. Zeng, X. Jiang, R. Li, D. Yuan, X. Ai, H. Yang, *Adv. Sci.* **2016**, *3*, 1.
- [73] H. Kaneko, K. Sekine, T. Takamura, *J. Power Sources* **2005**, *146*, 142.
- [74] K. Xu, U. Lee, S. Zhang, J. L. Allen, T. R. Jow, *Electrochim. Solid-State Lett.* **2004**, *7*, A273.
- [75] K. Xu, S. Zhang, T. R. Jow, *Electrochim. Solid-State Lett.* **2005**, *8*, A365.
- [76] K. Xu, S. Zhang, B. A. Poese, T. R. Jow, *Electrochim. Solid-State Lett.* **2002**, *5*, A259.
- [77] W. Xu, C. A. Angell, *Electrochim. Solid-State Lett.* **2001**, *4*, E1.
- [78] R. Mogensen, S. Colbin, A. S. Menon, E. Björklund, R. Younesi, *ACS Appl. Mater. Interfaces* **2020**, *3*, 4974.
- [79] B. Li, M. Xu, T. Li, W. Li, S. Hu, *Electrochim. Commun.* **2012**, *17*, 92.
- [80] H. Che, X. Yang, H. Wang, X. Z. Liao, S. S. Zhang, C. Wang, Z. F. Ma, *J. Power Sources* **2018**, *407*, 173.
- [81] H. Zhao, X. Yu, J. Li, B. Li, H. Shao, L. Li, Y. Deng, *J. Mater. Chem. A* **2019**, *7*, 8700.
- [82] J. Xia, L. Ma, J. R. Dahn, *J. Power Sources* **2015**, *287*, 377.
- [83] H. Che, J. Liu, H. Wang, X. Wang, S. S. Zhang, X.-Z. Liao, Z.-F. Ma, *Electrochim. Commun.* **2017**, *83*, 20.
- [84] H. Cai, H. Jing, X. Zhang, M. Shen, Q. Wang, *J. Electrochim. Soc.* **2017**, *164*, A714.
- [85] H. Liu, A. J. Naylor, A. S. Menon, W. R. Brant, K. Edström, R. Younesi, *Adv. Mater. Interfaces* **2020**, *7*, 2000277.
- [86] N. N. Sinha, J. C. Burns, J. R. Dahn, *J. Electrochim. Soc.* **2014**, *161*, A1084.
- [87] D. Y. Wang, J. Xia, L. Ma, K. J. Nelson, J. E. Harlow, D. Xiong, L. E. Downie, R. Petibon, J. C. Burns, A. Xiao, W. M. Lamanna, J. R. Dahn, *J. Electrochim. Soc.* **2014**, *161*, A1818.

- [88] D. Y. Wang, J. R. Dahn, *J. Electrochem. Soc.* **2014**, *161*, A1890.
[89] L. Ma, D. Y. Wang, L. E. Downie, J. Xia, K. J. Nelson, N. N. Sinha, J. R. Dahn, *J. Electrochem. Soc.* **2014**, *161*, A1261.
[90] O. Matsuoka, A. Hiwara, T. Omi, M. Toriida, T. Hayashi, C. Tanaka, Y. Saito, T. Ishida, H. Tan, S. S. Ono, S. Yamamoto, *J. Power Sources* **2002**, *108*, 128.
[91] D. Aurbach, K. Gamolsky, B. Markovsky, Y. Gofer, M. Schmidt, U. Heider, *Electrochim. Acta* **2002**, *47*, 1423.
[92] H. Ota, Y. Sakata, A. Inoue, S. Yamaguchi, *J. Electrochem. Soc.* **2004**, *151*, A1659.
[93] F. Lindgren, C. Xu, L. Niedzicki, M. Marcinek, T. Gustafsson, F. Björefors, K. Edström, R. Younesi, *ACS Appl. Mater. Interfaces* **2016**, *8*, 15758.
[94] M. Dahbi, N. Yabuuchi, M. Fukunishi, K. Kubota, K. Chihara, K. Tokiwa, X. Yu, H. Ushiyama, K. Yamashita, J.-Y. Son, Y.-T. Cui, H. Oji, S. Komaba, *Chem. Mater.* **2016**, *28*, 1625.
[95] G. Yan, K. Reeves, D. Foix, Z. Li, C. Cometto, S. Mariyappan, M. Salanne, J. Tarascon, *Adv. Energy Mater.* **2019**, *9*, 1901431.
[96] Y. Zheng, Y. Lu, X. Qi, Y. Wang, L. Mu, Y. Li, Q. Ma, J. Li, Y. S. Hu, *Energy Storage Mater.* **2019**, *18*, 269.
[97] P. Y. Zavalij, S. Yang, M. S. Whittingham, *Acta Crystallogr. Sect. B* **2003**, *59*, 753.

Manuscript received: October 27, 2020

Revised manuscript received: December 16, 2020

Accepted manuscript online: December 24, 2020

Version of record online: February 9, 2021